2010

Transepithelial D-glucose and D-fructose Transport Across Lobster Intestine

Ijeoma Ebelechukwu Obi
University of North Florida

Transepithelial D-glucose and D-fructose Transport across Lobster Intestine

by

Ijeoma Ebelechukwu Obi

A thesis submitted to the Department of Biology

in partial fulfillment of the requirements for the degree of

Master of Science in Biology

UNIVERSITY OF NORTH FLORIDA

COLLEGE OF ARTS AND SCIENCES

May, 2010

CERTIFICATE OF APPROVAL

The thesis of Ijeoma Ebelechukwu Obi is approved: (Date)

Signature deleted

09 April 10

Signature deleted

04/29/10

Signature deleted

4/29/2010

Committee Chairperson

Accepted for the Department:

Signature deleted

10 April 2010

Chairperson

Accepted for the College:

Signature deleted

10 MAY 2010

Dean

Accepted for the University:

Signature deleted

5/12/10

Dean of Graduate Studies

ACKNOWLEDGEMENTS

This work is supported by NSF grant IBN04-21986 and Doctor Gregory Ahearn. I would like to thank my major advisor, Dr. Gregory Ahearn for his guidance and support that allowed me to complete the graduate program here at the University of North Florida. I would also like to thank my graduate committee members, Dr. Judith Ochrietor and Dr. John Hatle for their support as well. In addition, I would like to thank the faculty and staff of the University of North Florida Biology Department for making my graduate experience very memorable.

I owe much gratitude to my parents Sampson Emenike Obi and Esther Ifeyinwa Obi for their prayers and support and also to my siblings Chika, Anulika and Ozioma Obi for being there for me throughout graduate school. Also, thank you to my fellow student researchers and friends. Most importantly, I would like thank God for giving me the wisdom, understanding, favor and health that I needed to complete my graduate program here at the University of North Florida.

TABLE OF CONTENTS

LIST OF TABLES AND FIGURES

ABSTRACT

The mechanisms of transepithelial absorption of dietary D-glucose and D-fructose in the American lobster, *Homarus americanus,* were investigated in this study in order to determine whether sugar transport proteins have been conserved throughout evolution. Whole lobster intestine was isolated and mounted in a perfusion chamber to determine transepithelial mucosal to serosal (MS) and serosal to mucosal (SM) mechanisms of ^{3}H-D-glucose and ^{3}H-D-fructose transport across the intestine. Unidirectional MS and SM fluxes were measured by adding variable concentrations of ^{3}H-D-glucose and ^{3}H-D-fructose (2.5 to 50μM) to either the perfusate or the bath respectively and sampling the amount of radioactivity that exited the opposite side of the intestine. Both the transepithelial MS and SM transports of ^{3}H-D-glucose and ^{3}H-D-fructose were hyperbolic functions of sugar concentration. The net flux of both sugars indicated a net absorption of D-glucose and D-fructose into the serosal compartment. Inhibitory analysis showed that while phloridzin decreased MS ^{3}H-D-glucose transport via a sodium glucose transport (SGLT 1-like) protein located on the mucosal membrane, ^{3}H-D-fructose transport was not affected by the drug. Mucosal phloretin decreased MS D-fructose transport but not MS D-glucose transport. Immunohistochemistry analysis revealed the presence of a mucosal GLUT 5 transport protein on the mucosal membrane. Increasing serosal concentrations of phloretin decreased both SM D-glucose and D-fructose transport suggesting the presence of a serosal GLUT 2 used by both sugars. The results of this study support the concept of conserved mechanisms of sugar transport in multicellular animals.

INTRODUCTION

Dietary sugars are the main source of energy in living organisms and they play an essential role in the proper functioning of organs (Wright and Hirayama, 2007). Most heterotrophic organisms use D-glucose, D-fructose and D-galactose as their main sources of carbon (Walmsley et.al. 1998). The biological membrane of organs is selectively permeable, allowing the passage of small molecules and lipid-soluble substances to pass through the hydrophobic interior of the plasma membrane. For example, certain molecules such as gases, small polar molecules like glycerol, and larger non-polar molecules like hydrocarbons can easily pass through the lipid membrane (Raven et al., 2008). In addition, some larger polar molecules like glucose and charged molecules can pass through the lipid membrane much slower. The lipid portion of the membrane is relatively impermeable to ions, large, and small polar molecules like sugars; and as a result, certain integral membrane proteins are involved in the transport of these molecules into and out of cells (Raven et al., 2008). Transport occurs via passive and active mechanisms. Therefore the two types of transport proteins that were investigated in this study are facilitated diffusion carrier transport proteins and active transport proteins.

Facilitated diffusion transport mechanisms involve proteins that are capable of transporting certain ions and molecules across the membrane and are dependent on a concentration gradient (Raven et al., 2008). In other words, facilitated diffusion is the net movement of molecules or ions from a region of high concentration to a region of low concentration. On the other hand, active transport involves a pump that uses metabolic energy to function, and transports ions and molecules against their concentration

gradients. There are two major types of active transport: primary and secondary active transport. The sodium-potassium pump is an example of primary active transport in which there is an unequal exchange of three sodium ions exported out of the cell for two potassium ions that is imported into the cell. This process requires the expenditure of energy leading to the generation of an electrical gradient across the plasma membrane (Raven et al., 2008). This means that the driving forces for actively transporting ions and molecules across the plasma membrane are both the concentration gradient and the electrical potential. Secondary active transport, on the other hand, uses a transport protein that indirectly utilizes the sodium-potassium pump to transport ions and molecules across the plasma membrane (Raven et al., 2008). In glucose transport for example, the sodium exported from the cell, using the sodium-potassium pump, is transported back into the cell and down its concentration gradient in conjunction with glucose using a specific glucose transporter.

Absorption of glucose has been extensively studied in mammals, leading to the findings that two distinctly different types of sugar transport proteins have evolved to transfer this nutrient across membranes of living organisms. These transporters include the SLC5 co-transporter gene family and the SLC2A gene family (Wood and Trayhurn, 2003). The SLC5 co-transporter gene family is a large family of 75kDa proteins consisting of several sodium/glucose cotransporter (SGLT) proteins that transport glucose across biological membranes. SGLT transport proteins are powered by transmembrane ion gradients which transport glucose in conjunction with sodium into the cytosol of both eukaryotic and prokaryotic cells. Of all the SGLT transport proteins, the SGLT 1 transporter is the best studied member of the SLC5 gene family and it is present

in the apical membrane of the mammalian intestine. The SGLT 1 transport protein is made up of 14 transmembrane α-helices that span the plasma membrane with both the N and C termini facing the extracellular side of the membrane (Fig. 1A) (Wright et al., 2007). Functional studies of the SGLT protein indicated that the sugar binding region is located in the C-terminal portion of the protein (Wright et al., 2007).

On the other hand, the SLC2A gene family is a family of 50kDa proteins. They are composed of glucose transport proteins (GLUT) that act as facilitated diffusion systems. Unlike the SGLT family, members of the GLUT family possess 12 transmembrane α-helices with both the N and C termini facing the intracellular side of the plasma membrane (Fig. 1B) (Manolescu et al., 2007). These 12 transmembrane α-helices combine together to form a channel through which substrates are able to cross the lipid membrane (Fig. 1B) (Manolescu et al., 2007). The ability of the GLUT proteins to transport glucose or fructose depends on the amino acid residues present on the translocation channel (Manolescu et al., 2007). GLUT 2 is the carrier protein that is inserted in the luminal side of the intestinal epithelial cell and is responsible for uptake of luminal glucose in the presence of high concentration of glucose, while GLUT 5 is the known carrier responsible for luminal fructose transport (Caccia et al., 2007). Also, GLUT 2 is present on the basolateral membrane and is responsible for bringing in both glucose and fructose from the blood into the cytosol (Caccia et al., 2007).

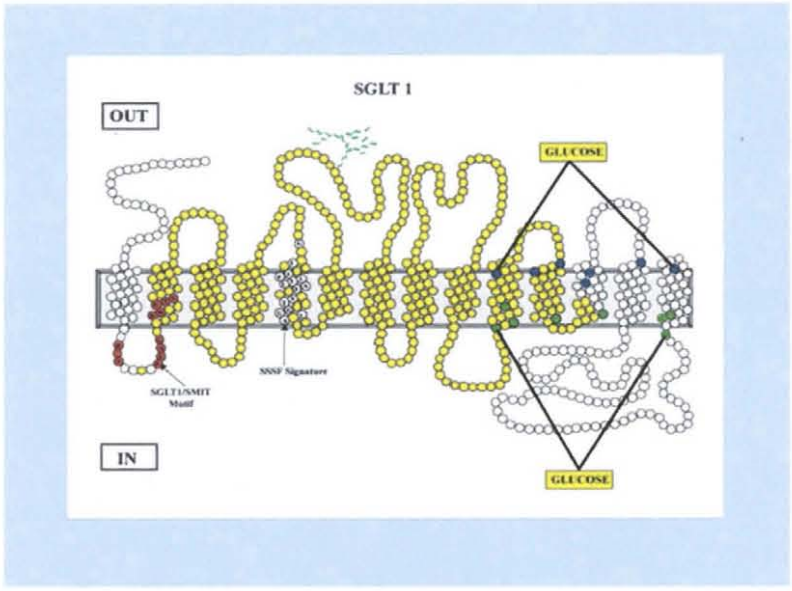

A

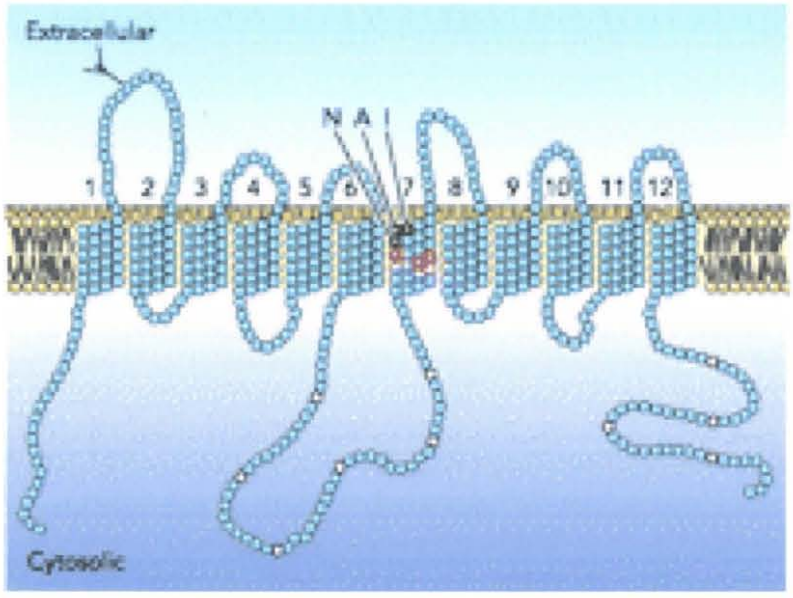

B

Figure 1: Structural models for SGLT 1and GLUT transport proteins. Fig. A represents the 14 transmembrane α-helices with extracellular N- and C- termini of SGLT transport protein. Fig. B represents the 12 transmembrane α-helices with intracellular N- and C-termini of the GLUT transport proteins (Wright et al., 2007; Manolescu et al., 2007).

While sugar transporters have been extensively studied in mammals, very little is known about absorption of sugars in invertebrates. In crustaceans, the hepatopancreas and the intestine have been shown to play a role in the absorption of dietary glucose (Verri et al., 2001) with the hepatopancreas being the major site of sugar absorption (Ahearn and Maginniss, 1976; Chu, 1986). There are three major parts to the crustacean digestive tract: the foregut, the midgut and the hindgut. The foregut is the portion of the intestine that is closer to the mouth of the animal while the hindgut is the portion closer to the tail of the animal. The midgut, located in between the foregut and hindgut, consists of the intestine and the hepatopancreas and these organs play the major role in nutrient absorption; on the other hand, the foregut and hindgut have a very little role in nutrient absorption (Wright and Ahearn, 1997). The hepatopancreas is a large, bilateral organ that is composed of 5 different cell types: E, F, R, B and M cells (Verri et al., 2001). Each of the cell types differ in their cell structure and as a result play different roles in digestive functions (Verri et al., 2001). On the contrary, the intestine is made up of a single type of epithelial cell. The study of an organ with a single cell type is important because it allows scientists to accurately make conclusions about cellular mechanisms occurring in an organism. In the American lobster, *Homarus americanus*, the intestine is considered a scavenger organ that absorbs nutrients that were not taken up by the hepatopancreas. A picture of a dissected lobster showing the position of the intestine and the hepatopancreas is shown in Fig. 2.

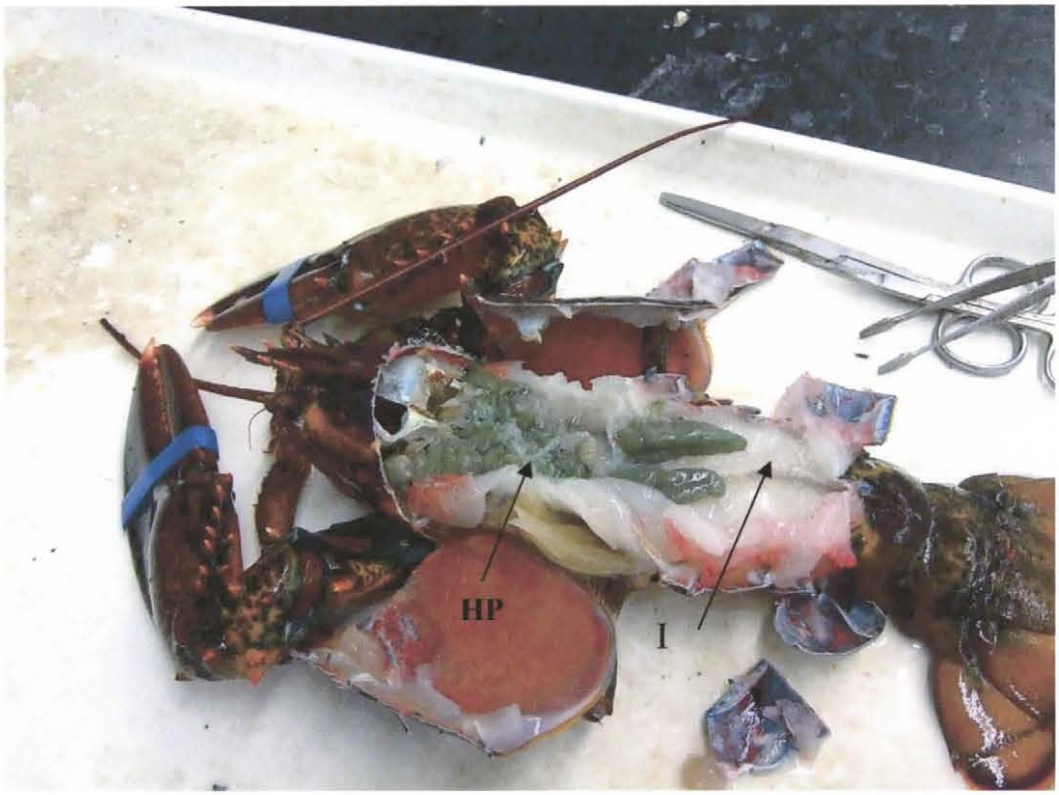

Figure 2: A dissected lobster showing the bilobed hepatopancreas HP and the intestine I. Part of the intestine lies underneath the hepatopancreas and runs through the tail of the lobster. This picture was taken at the University of North Florida Physiology Research Laboratory, Jacksonville, Fl.

Some research on sugar transport in bacteria and protozoans has been conducted as well. Sugar transport in *E. coli* is evolutionary closer to mammalian transporters (Maiden et al., 1987 and Henderson et al., 1990) than to those of the eukaryotic parasitic protozoan, *Trypanosoma brucei*, the causative agent of the African sleeping sickness (Tetaud et al., 1997). Both *E. coli* and the parasitic protozoan sugar transporters belong to the superfamily termed the major facilitator (MF) superfamily (Walmsley et al., 1998).

In *E.coli*, sugars are transported across the cell membrane via proton-dependent transporters such as the GalP, AraE, and XylE transport proteins which transport D-glucose/D-galactose, arabinose and xylose, respectively (Walmsley et al., 1998). This mechanism of sugar transport in *E. coli* is similar to the SGLT transport proteins in mammals in the sense that an ion is used to transport glucose across the membrane (Turk et al., 1996). In *E. coli*, glucose is co-transported across the membrane using H^+ (Henderson, 1990), unlike Na^+ in mammals (Turk et. al 1996). Parasitic protozoans, the kinetoplastida, also have sugar transporters that are members of the MF superfamily (Walmsley et al., 1998). These groups of organisms include *Trypanosoma brucei*, which cause sleeping sickness and *Trypanosoma cruzi* which causes Chagas disease (Tetaud et al, 1997; Walmsley et al., 1998). Much work has been done to understand the structure of the sugar transporter (THT1) in *Trypanosoma brucei* to develop a chemotherapeutic drug for killing the parasite (Tetaud et al, 1997). Sleeping sickness is transmitted to humans by tsetse flies. *Trypanosoma brucei* has evolved distinct sugar transporters due to its two separate life stages: in the midgut of the tsetse fly and in the mammalian bloodstream (Tetaud et al, 1997). In the human bloodstream where there is a relatively high concentration of glucose, the parasite has evolved a low affinity sugar transporter, but in the midgut of the tsetse fly, a high affinity sugar transport is present to meet the metabolic demands of the parasite in a low sugar environment (Tetaud et al, 1997).

A comparison of the facilitated sugar transporters of members of the MF superfamily and mammalian sugar transporters reveals similarities in the primary structures of the sugar transport proteins (Walmsley et al., 1998). The facilitated diffusion carrier proteins of both mammals and members of the MF suparfamily are similar in

several ways. First, both transport proteins contain 12 transmembrane α-helices with both the N- and C- terminals facing the intracellular side of the plasma membrane (Walmsley et al., 1998). Second, both sugar transport proteins have inward and outward sugar binding sites (Walmsley et al., 1998). The transport of sugar across the plasma membrane is made possible as the transporter undergoes conformational changes in which binding of the sugar on one side of the membrane leads to closing of the opposite end (Walmsley et al., 1998). Finally both sugar transporters have specific amino acid residues that play crucial roles in the binding of substrates. For example, in mammals, the replacement of the amino acid isoleucine with valine leads to loss in the transport of D-fructose (Manolescu et al., 2005), while for members of the MF superfamily, replacement of tryptophan located in the amino acid position 412 with leucine decreased glucose transport (Walmsley et al., 1998).

Sugar transport mechanisms have also been studied in insects. *Aphid ervi* is a parasitic wasp that lays its eggs in the haemocoel of a different species of aphids (Caccia et al., 2007). The larval development of the insect occurs in the hemolymph of its host (Caccia et al., 2007). In a study conducted on the midgut of *Aphid ervi*, apical and basolateral fluxes of D-glucose and D-fructose, in addition to immunocytochemistry and western blot analysis were used to determine the localization of sugar transport proteins on the midgut epithelial plasma membranes (Caccia et al., 2007). The results obtained revealed the localization of SGLT 1 and GLUT 5 on the apical membrane (Caccia et al., 2007). GLUT 2 was shown to be present on the basolateral side of the gut and in the presence of high concentration of sugars, GLUT 2 was inserted into the apical side of the membrane to maximize uptake of the sugars (Caccia et al., 2007). The findings by Caccia

et al., (2007) are important because they are the only known non-vertebrate eukaryote studies that support the evolutionary conservation of sugar transporters in eukaryotic organisms.

Apart from the above parasitic study conducted in insects, sugar transport mechanisms have not been studied in depth in any free living eukaryotic organism. In this study, the American lobster, *Homarus americanus,* was chosen because of its position on the phylogenetic tree between parasitic protozoans and vertebrate eukaryotes, and also because of its significant divergence from mammals. It was hypothesized that sugar transporters must be highly conserved throughout evolution because the glucose molecule is the same for all organisms that use it for energy; hence transepithelial sugar transport in crustaceans is expected to be similar to the standard model proposed in mammals. The intestinal mammalian sugar transport proteins are shown in Fig. 3.

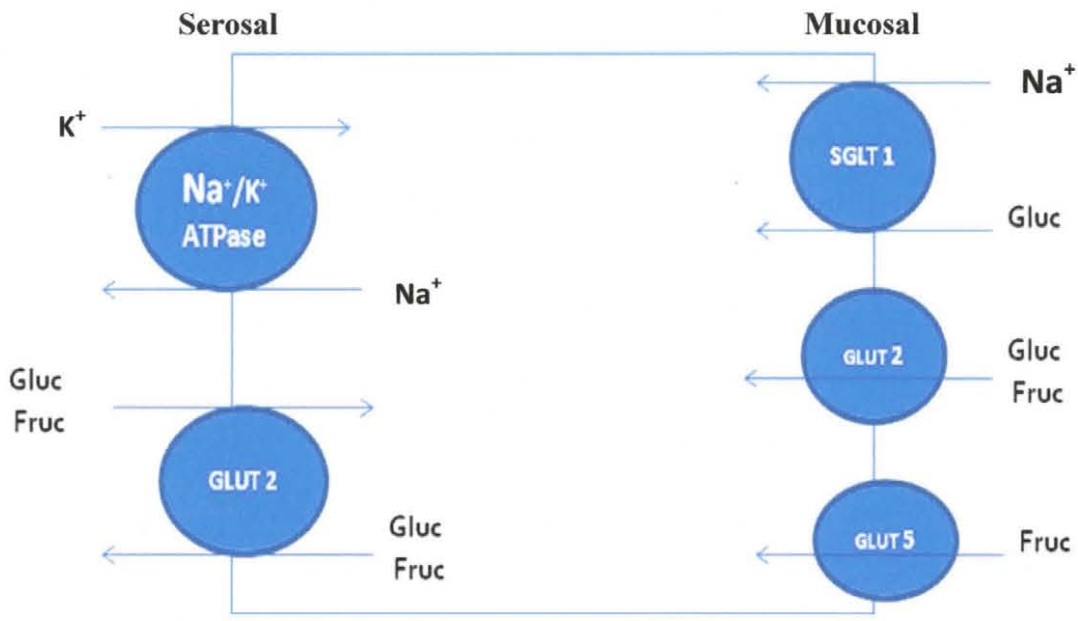

Figure 3: Standard model for sugar transport proteins in the mammalian intestinal cells (Kellet, 2001). On the mucosal membrane is the SGLT 1 transport protein responsible for translocation of glucose into the cell in conjunction with sodium; GLUT 2 protein is involved in transport of both glucose and fructose into the cell; and GLUT 5 protein is specific for transport of fructose into the cell. On the serosal side is a GLUT 2 protein involved in transport of both glucose and fructose in and out of the cell. The sodium/potassium pump supplies Na^+ needed for transporting mucosal glucose into the cell via the SGLT 1 protein.

MATERIALS AND METHODS

Animals

Live, male lobsters, *Homarus americanus*, were purchased from a local seller (Fisherman's dock, Jacksonville, Florida). Each lobster weighed approximately 0.5kg and was kept in a tank containing fresh seawater at 15°C. Animals were fed half pound frozen mussel meat twice a week until needed for an experiment.

Mucosal to Serosal (MS) Transport

In vitro transmural transports of ^{3}H-D-glucose and ^{3}H-D-fructose were studied using a perfusion apparatus as previously described by Ahearn and Maginniss (1976) (Fig. 4). Isolated whole intestine was flushed with physiological saline (410mM NaCl, 15mM KCl, 5mM $CaSO_4$, 10mM $MgSO_4$, 5mM $NaHCO_3$, and 5mM Hepes; an addition of KOH was used to obtain a pH of 7.1) and mounted on an 18-20 gauge needle at both ends of the perfusion apparatus using a surgical thread. The length and diameter of the experimental intestine was measured and the intestinal surface area was calculated using the equation: $A = \Pi ld$, where "l" and "d" represents the length and diameter of the intestine, respectively. The perfusion bath (serosal medium) was filled with 35mL of physiological saline. Experimental perfusate was pumped through the intestine using a peristaltic pump, (Instech Laboratories, Inc., Plymouth Meeting, PA, USA), at a rate of 0.38mL min^{-1}. Time course kinetics experiments were conducted by adding experimental concentrations of D-glucose or D-fructose to different 50mL tubes (Falcon, Newark, DE) containing 20µL of ^{3}H-D-glucose or 10µL of ^{3}H-D-fructose respectively depending on

the experimental protocol. Prior to the start of experimentation, triplicate aliquots of each perfusate (200μL) were collected from each Falcon tube and from the bath to determine the total count of radioactively labeled sugar in each tube and the amount of background radioactivity in the bath. An equal amount of saline as were removed from the bath was replaced to maintain a constant volume in the bath. Experimental solutions were then perfused through the intestine for a total of thirty minutes at each concentration of sugar. The perfusate of inhibition experiments contained the experimental concentration of D-glucose or D-fructose, ^{3}H-D-glucose or ^{3}H-D-fructose and inhibitors such as phloretin and phloridzin. The solutions were perfused through the intestine for the duration of each treatment. All experimental procedures were carried out at room temperature (23°C). For both time-course and inhibition experiments, triplicate aliquots of radioactive samples (200μl) were obtained from the serosal medium after passage across the intestine every five minutes for the duration of each experimental treatment. An equal amount of saline was replaced in the serosal medium in order to maintain a constant volume in the bath.

Serosal to Mucosal (SM) Transport

In vitro transmural serosal to mucosal transport of ^{3}H-D-glucose and ^{3}H-D-fructose was similarly studied. In this case, time course kinetics experiments were conducted by adding the corresponding radioactively labeled sugar required for each experiment to the bath. The total amount of radioactivity in the bath was determined by collecting triplicate samples of 200μL of solution from the bath. During experimentation, physiological saline was perfused through the intestine and an increased experimental concentration of the sugar was added to the bath after every thirty minutes. A single

sample of radioactive ^{3}H-D-glucose or ^{3}H-D-fructose exiting the intestine into the prefusate was collected every five minutes, for the duration of the experiment, into a 7mL tube containing 3mL of scintillation cocktail.

Data Analyses

Each experimental sample was placed in a 7mL tube containing 3mL scintillation cocktail and counted for radioactivity in a Beckman LS6500 scintillation counter. The amounts of radioactivity in each tube for both MS and SM experiments were reported in counts per minute (cpm). An average of the background counts were subtracted from each triplicate sample at each time point. Transmural flux rates expressed in pmol/cm^2 x min for MS experiments were calculated by taking the average of the samples during each time period, while taking into account intestinal surface area and dividing by the isotope specific activity for each concentration. Slopes of the time course data were determined using linear regression and data curve fitting analysis were performed using Sigma Plot software (Systat Software inc., Point Richmond, CA, USA). Bar graphs were obtained by plotting flux rate as a function of experimental treatment and are expressed in pmol/cm^2 x min. Experiments were repeated two or three times providing qualitatively similar results between animals.

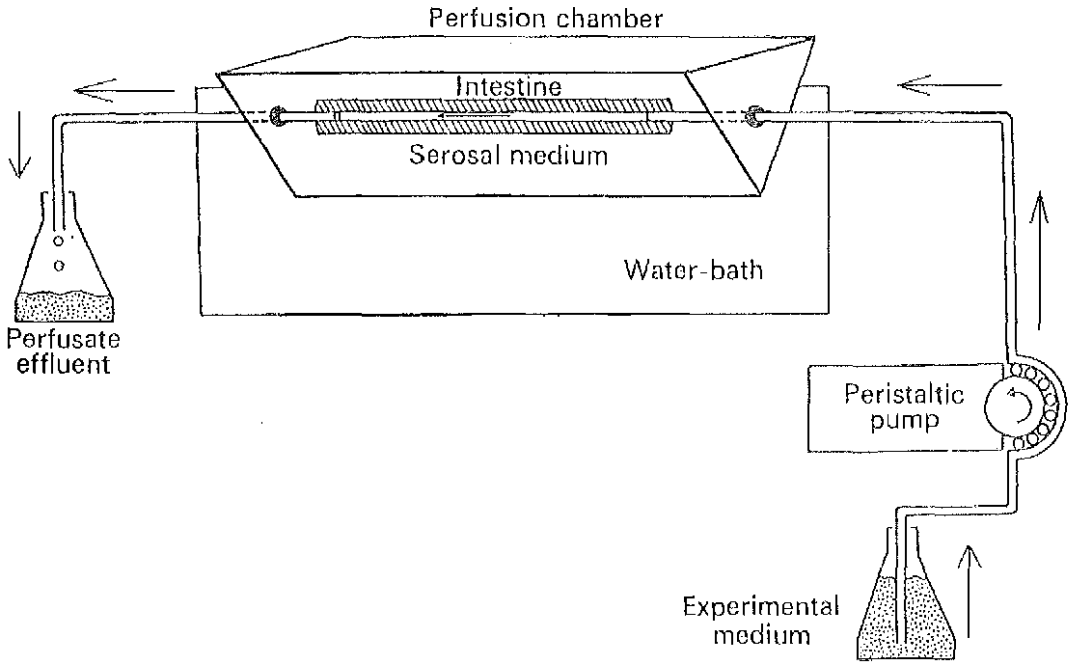

Figure 4: A diagram of the perfusion apparatus used to measure ^{3}H-D-glucose and ^{3}H-D-fructose transport by the lobster intestine, *Homarus americanus* (Ahearn and Maginniss, 1976). The serosal/basolateral medium represents the blood side while the mucosal/apical medium represents inside the intestine.

Tissue Preparation, Dehydration, Embedding and Sectioning

Whole lobster intestines were isolated and were dissected into small pieces in cross section. Sections were placed in 10% buffered formalin and stored at room temperature for about 3-4 days. Each sections was dehydrated by placing it in a separate vial containing one of several concentrations of aqueous ethyl alcohol and three changes of citrisolv (70, 80, 95, 95, 100,100% ethyl alcohol, citrisolv in order) for one hour at each exposure. Tissues were then placed in a 50/50 citrisolv: paraffin mix overnight at 57^0C. Intestines were removed from the mix and placed in paraffin at 57^0C for 1hour after which each intestinal piece was crossectionally embedded in a plastic block covered with paraffin and was allowed to cool at room temperature overnight. Excess paraffin was trimmed off from the face of the blocks and the lobster tissues were cut into ribbons of 7μm thickness using a microtome and placed onto a water bath at 37^0C. Each ribbon was picked and positioned on a labeled glass slide and each slide was placed on a slide warmer at 60-65^0C for about 30-35 minutes. After tissues had adhered to the slides, the slides were then placed in a slide box and stored at room temperature for processing.

Rehydration

Prior to staining, tissue sections were re-hydrated by placing each tissue slide in different vials containing citrisolv and several concentrations of aqueous ethyl alcohol (citrisolv1, 2 and 3, 100, 100, 95, 95, 80, 80, 70% ethyl alcohol in order) for 5 minutes at each exposure. After exposure to 70% ethyl alcohol, the slides were held in water for 2 to 3 minutes before staining.

Masson Trichrome Staining

Rehydrated slides were placed in the following solutions: Bouin's fluid at 56^0C for 1 hour, Wrigert's iron hematoxylin stain for 10 minutes, Biebrich scarlet acid fuchsin solution for 5 to 10 minutes until desired intensity was achieved, phosphotungstic-phosphomolybdic acid solution for 5 minutes, aniline blue stain solution for 5 to 10 minutes to achieve desired intensity and, 1% acetic acid solution for 1 minute. The slides were rinsed with tap water in between each solution. After the slides were placed in acetic acid solution, they were rinsed in distilled water and dehydrated in two changes of anhydrous alcohol for 1 minute each. Slides were then placed in three changes of citrisolv for 1 minute and cover slips were placed on each slide using parmount for storage. Pictures of the slides were taken using an Olympus BX60 microscope.

Immunohistochemistry

Rehydrated slides were incubated in pre-incubation buffer (TBS and 2% normal goat serum) at room temperature for 1 hour to block non specific binding. Next, the slides were washed in TBS three times and then incubated overnight at 4°C in 1:100 rabbit polyclonal, primary antibody to GLUT 5 diluted in pre-incubation buffer. After incubation, the slides were washed in TBS 3 times and then incubated in the dark for 1 hour in 1:100 goat anti rabbit secondary antibody conjugated with FITC diluted in pre-incubation buffer. Vector shield was used to place cover slips on the slides for storage. Pictures of the slides were taken using an Olympus BX60 microscope. Negative controls were not incubated in primary antibody. The difference between the intensity of fluorescence on the mucosal and serosal aspect of the villi-like projections was analyzed

using Kodak Molecular Imaging Software (Carestream Health Inc., Rochester, NY, USA). The mean intensities of thirty randomly sampled areas on the mucosal aspect of the projection were compared to an equal number of randomly sampled areas on the serosal aspect of the projection. Student's T-test was used to determine significant differences between the mean fluorescence intensities of both the mucosal and the serosal aspect of the villi-like projections.

RESULTS

^{3}H-D-glucose and ^{3}H-D-fructose Transport Kinetics

In order to determine the presence of a mucosal and serosal transporter, transmural ^{3}H-D-glucose was studied in the presence of increasing mucosal and serosal concentrations of D-glucose. The effect of increasing mucosal D-glucose on MS ^{3}H-D-glucose transport and increasing serosal D-glucose on SM ^{3}H-D-glucose transport are shown in Fig. 5 and 6 respectively. Time course analysis of ^{3}H-D-glucose transport was determined by taking triplicate samples every five minutes at each concentration for a duration of thirty minutes. Each data point represents pmoles/cm^{2}. Fig. 5 and 6 showed that the transport rates of ^{3}H-D-glucose were greater in MS uptake experiments than in SM uptake experiments. When MS and SM ^{3}H-D-glucose transport rates were plotted as a function of mucosal and basolateral glucose concentrations, the graph indicated that increasing concentration of luminal glucose increased ^{3}H-D-glucose transport in a hyperbolic manner (Fig. 7). Each data point represents the slope ± SEM at each

concentration of D-glucose, as shown in Fig. 5 and 6. Net flux was calculated by subtracting SM flux from MS flux at each concentration. The net flux of ^{3}H-D-glucose suggests an overall absorption of glucose by the intestine (Fig. 7). Also, the hyperbolic curve for both MS and SM ^{3}H-D-glucose transport indicated the presence of D-glucose transport proteins on both the mucosal and serosal sides of the intestine.

Kinetic constants are listed in Table 1. K_m is the concentration at which the transporter is working at half its maximum speed while J_{max} represents the maximum transport velocity of the substrate. A smaller K_m implies that the transporter has a higher binding affinity to the substrate. A high J_{max} suggests an accumulation of the sugar in the cell. MS and SM ^{3}H-D-glucose transport had similar K_m values but the J_{max} values of MS ^{3}H-D-glucose transport were about 4 times more than those of SM ^{3}H-D-glucose transport (Table 1).

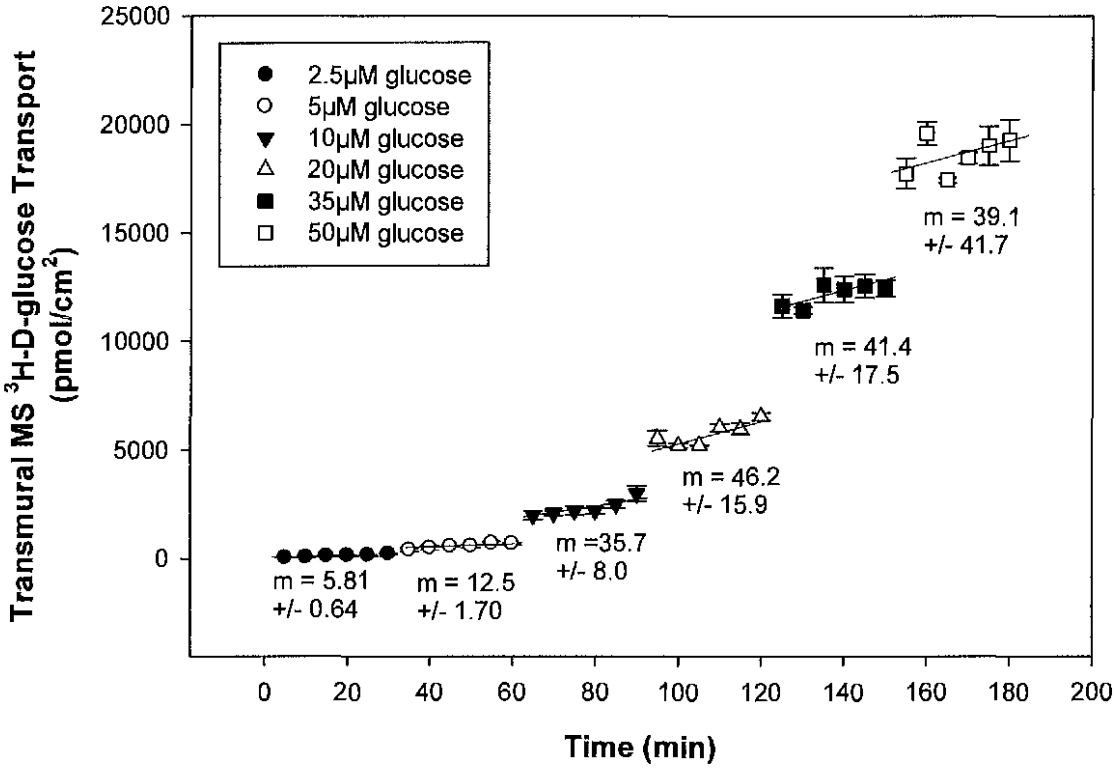

Figure 5: A time course experiment showing the effect of increasing mucosal D-glucose concentration on MS ^{3}H-D-glucose transport. Each individual data point represents the mean of ± SEM of three replicate samples per time point. Symbols are pmoles/cm^2 for each concentration of glucose. Transmural MS flux at each concentration is the calculated slope ± 1 SEM, which represents pmoles/cm^2 x min.

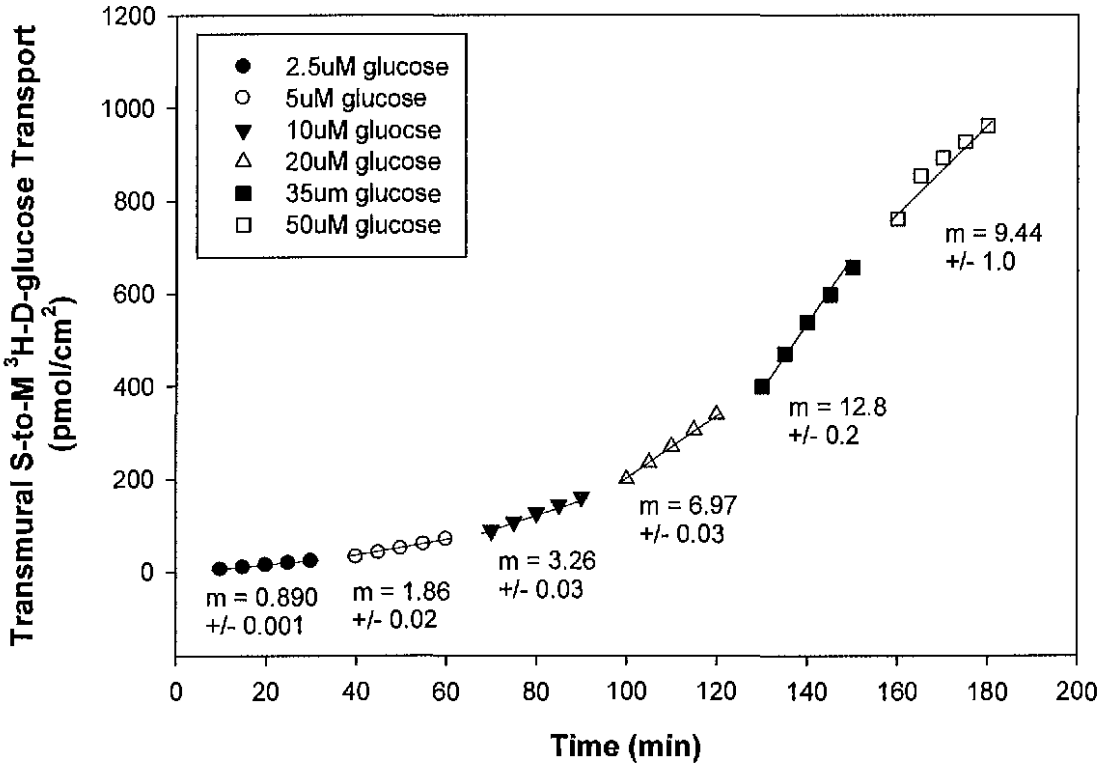

Figure 6: A time course experiment showing the effect of increasing serosal D-glucose concentration on SM ^{3}H-D-glucose transport. Symbols are pmoles/cm^2 for each concentration of glucose. Transmural SM flux at each concentration is the calculated slope ± 1 SEM, which represents pmoles/cm^2 x min.

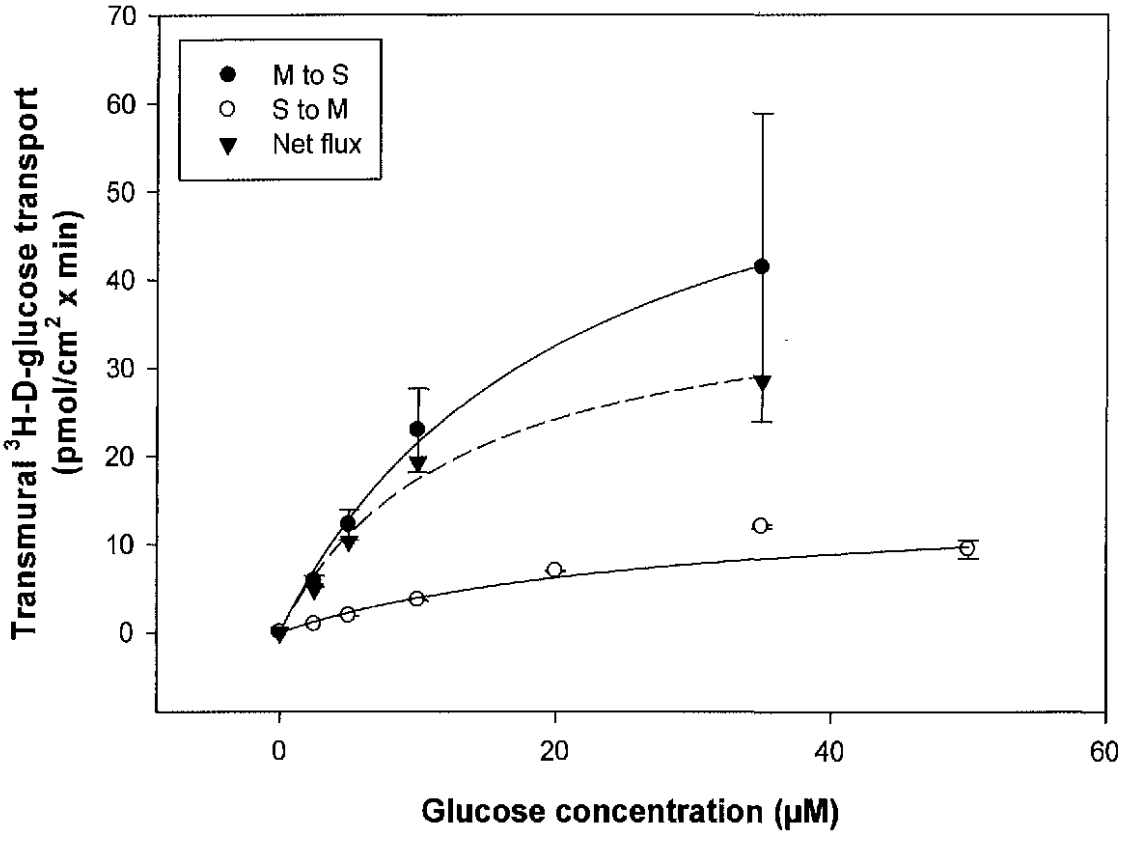

Figure 7: Effect of increasing D-glucose concentration on MS and SM transmural ^{3}H-D-glucose transport. Net flux represents the difference between MS and SM transport of ^{3}H-D-glucose. Data points for MS and SM plots are taken from Fig. 3 and 4. Kinetic constants are displayed in table 1.

Table 1: Comparison of MS and SM kinetic constants for ^{3}H-D-glucose and ^{3}H-D-fructose transmural transport.

Substrate	**J_{max} (pmol/cm^2 x min)**	**K_m (μM)**
MS ^{3}H-D-glucose	66 ± 4.7	21 ± 3.0
MS ^{3}H-D-fructose	6 ± 0.14	11 ± 0.73
SM ^{3}H-D-glucose	15 ± 1.9	29 ± 7.3
SM ^{3}H-D-fructose	3 ± 0.29	13 ± 3.9

Values are means ± 1 SEM from triplicate observations. Kinetic constants were obtained using Sigma 10.0 curve fitting software.

Mucosal and serosal transmural ^{3}H-D-fructose transport was studied similarly. The effects of increasing mucosal D-fructose concentration on MS ^{3}H-D-fructose transport and increasing serosal D-fructose concentration on SM ^{3}H-D-fructose transport are shown in Figure 8 and 9 respectively. Time course analysis of ^{3}H-D-fructose transport was determined as described above. Similar to glucose transport, MS transport of ^{3}H-D-fructose was also greater than SM transport of ^{3}H-D-fructose. An analysis of MS and SM transport rates plotted against mucosal and basolateral concentrations of D-fructose also showed hyperbolic curves (Fig. 10). Net flux of ^{3}H-D-fructose (MS-SM) was absorptive. Although both MS and SM transport of ^{3}H-D glucose and ^{3}H-D-fructose exhibited hyperbolic curves, it was clear that the transport rates of both MS and SM ^{3}H-D-glucose were greater than MS and SM transport rates of ^{3}H-D-fructose respectively (Figs. 7 and 10). Kinetic constants of MS and SM transport rates of ^{3}H-D-glucose and ^{3}H-D-fructose are shown in Table 1. Similar to glucose transport, MS and SM ^{3}H-D-fructose transport had similar K_m values but the J_{max} values of MS ^{3}H-D-fructose transport was about 2 times more than SM ^{3}H-D-fructose transport (Table 1).

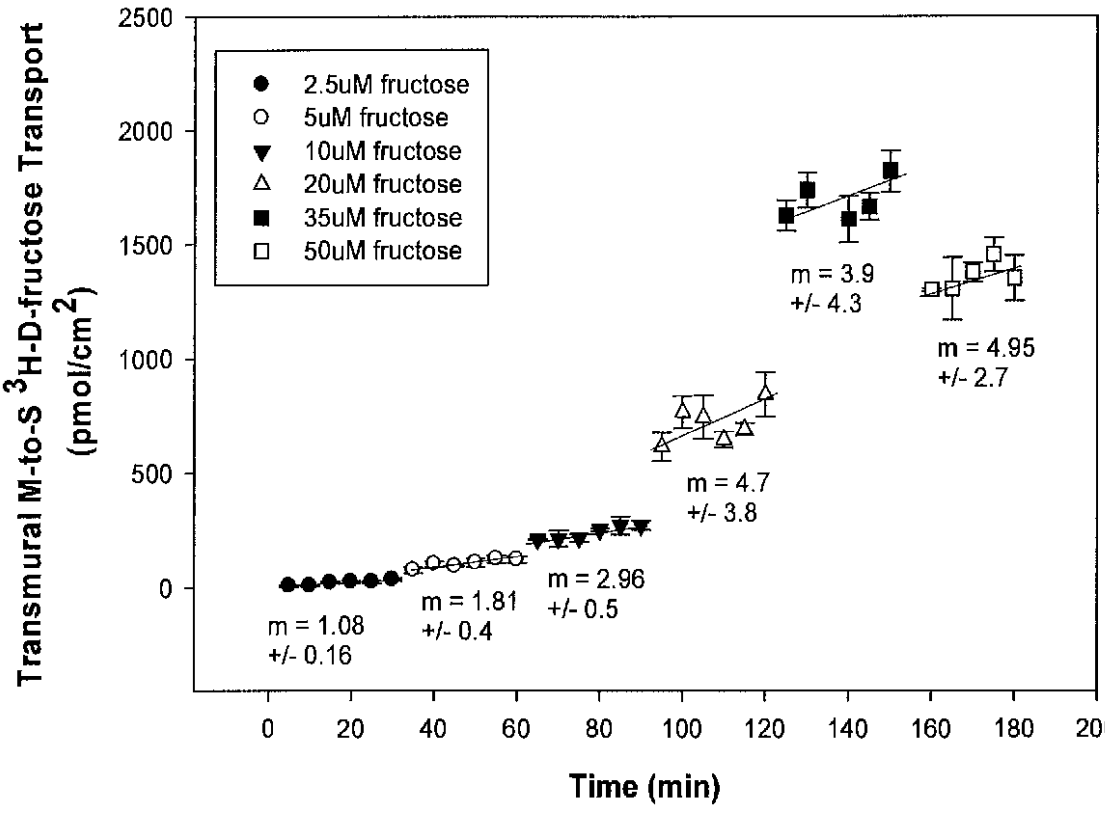

Figure 8: A time course experiment showing the effect of increasing mucosal fructose concentration on MS ^{3}H-D-fructose transport. Each individual data point represents the mean of ± SEM of three replicate samples per time point. Symbols are pmoles/cm^2 for each concentration of fructose. Transmural MS flux at each concentration is the calculated slope ± 1 SEM, which represents pmoles/cm^2 x min.

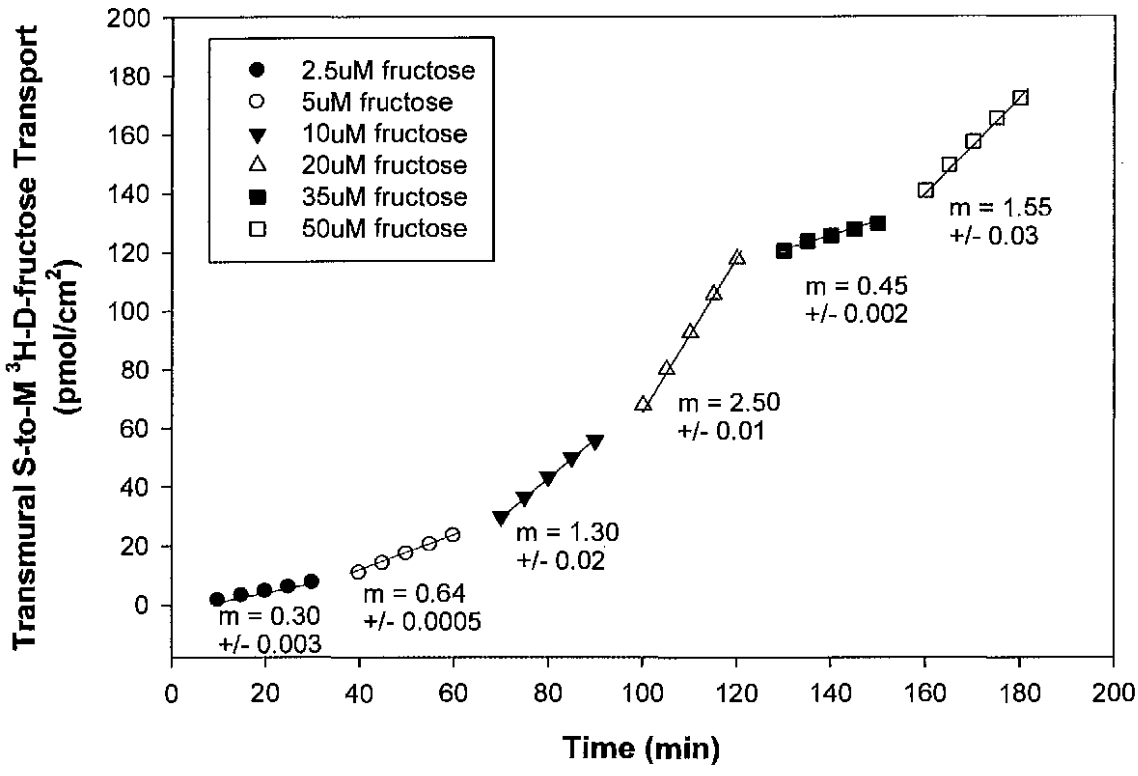

Figure 9: A time course experiment showing the effect of increasing serosal fructose concentration on MS ^{3}H-D-fructose transport. Symbols are pmoles/cm^2 for each concentration of fructose. Transmural SM flux at each concentration is the calculated slope ± 1 SEM, which represents pmoles/cm^2 x min.

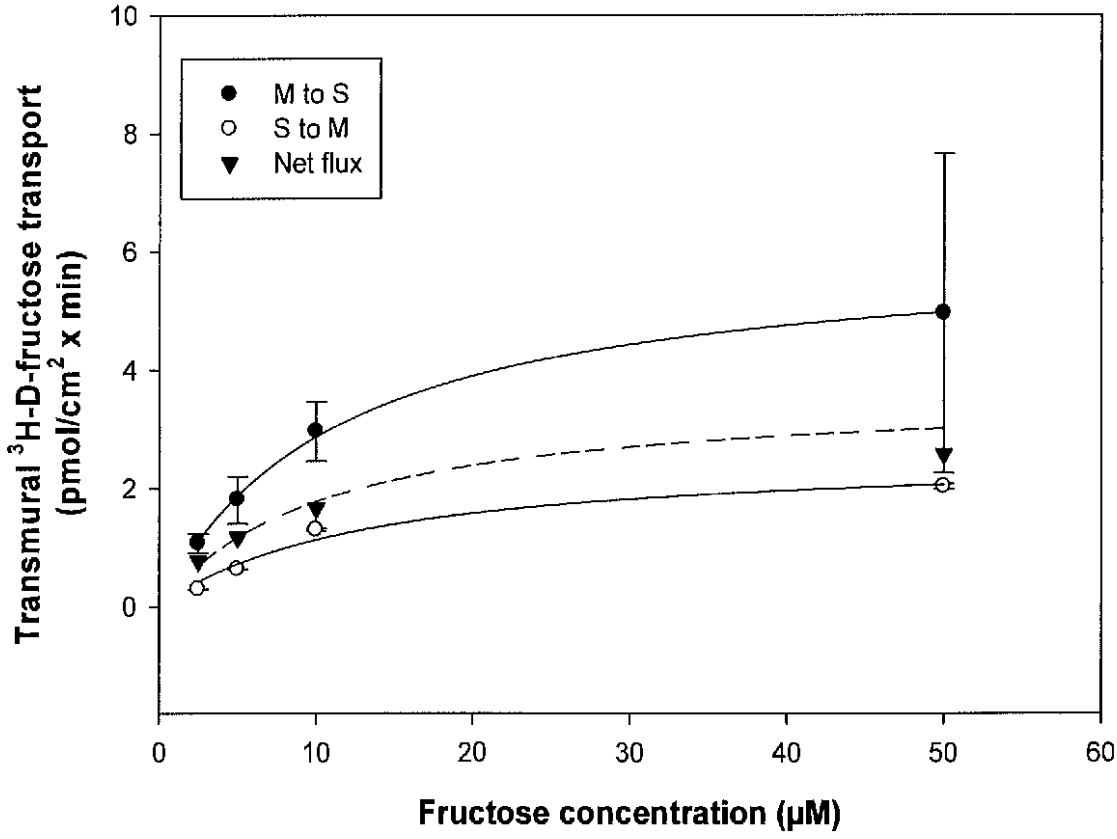

Figure 10: Effect of increasing D-fructose concentration on MS and SM transmural ^{3}H-D-fructose transport. Net flux represents the difference between MS and SM transport of ^{3}H-D-fructose. Data points for MS and SM plots are taken from Fig. 6 and 7. Kinetic constants are displayed in table 1.

Effect of phloridzin and phloretin on MS ^{3}H-D-glucose and MS ^{3}H-D-fructose Transport

The inhibitors, phloridzin and phloretin dissolved in 100% ethanol were used to determine the possible presence of SGLT 1-like and GLUT 2- like transporters on the mucosal membrane. Phloridzin is a known inhibitor of the SGLT 1 Na^{+}/glucose cotransporter located on the musosal membrane, while phloretin is an inhibitor of glucose and fructose transport via the GLUT 2 transport protein. The concentration of 25μM D-glucose and D-fructose was chosen for experimentation because at that concentration, both sugars have not reached their maximum transport rate. This means that the effect of the inhibitors could be easily observed since the sugar transporters are not saturated. When 25μM MS ^{3}H-D-glucose uptake was treated with 100μM phloridzin, the data showed a decrease in transmural 25μM ^{3}H-D-glucose transport (Fig. 11). In Fig. 11A, ^{3}H-D-glucose transport by animal 1 decreased by 68% while in Fig. 11B ^{3}H-D-glucose transport by animal 2 decreased by 64%. In addition, 100μM phloridzin did not inhibit 25μM ^{3}H-D-fructose transport (Figs. 13A and 13B). Phloridzin was dissolved in 100% ethanol. Transport of 25μM D-glucose and 25μM D-fructose was not affected in the presence of 100% ethanol (Figs. 11 and 13). These data suggests the presence of a mucosal SGLT 1 transport protein that is responsible for transport of ^{3}H-D-glucose but not ^{3}H-D-fructose.

Furthermore, transmural transport of 25μM MS ^{3}H-D-glucose in the presence of 100μM phloretin was not inhibited and ethanol did not significantly affect 25μM ^{3}H-D-glucose transport (Figs. 12A and 12B). The addition of 100μM mucosal phloretin

decreased 25μM MS ^{3}H-D-fructose transport (Fig. 14A and Fig 14B). In Figs. 14A, ^{3}H-D-fructose transport by animal 1 was decreased by 30% while in Fig. 14B ^{3}H-D-fructose transport by animal 2 was decreased by 58%. As before, ethanol did not affect 25μM MS ^{3}H-D-glucose and ^{3}H-D-fructose transport (Figs. 12 and 14). These data suggest the presence of a mucosal GLUT 2 transport protein responsible for transport of ^{3}H-D-fructose but not ^{3}H-D-glucose.

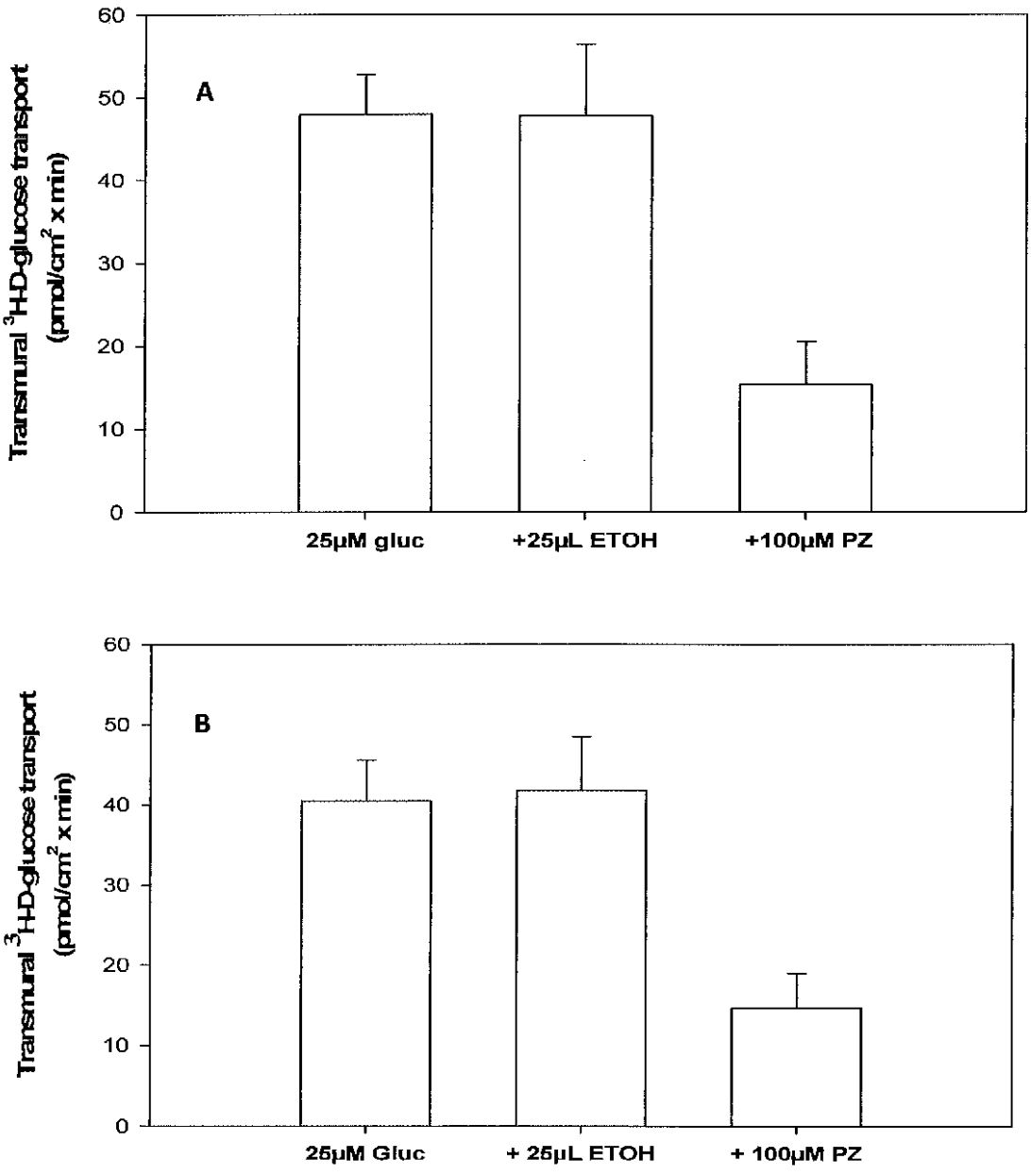

Figure 11: Effect of mucosal 100µM phloridzin on 25µM MS ^{3}H-D-glucose transport. Bar graphs are the slopes ± 1 SEM of triplicate replicates at each time point obtained from the time course data. Panels A and B are results obtained from different experiments using individual animals. Phloridzin was dissolved in ETOH before adding to incubation medium.

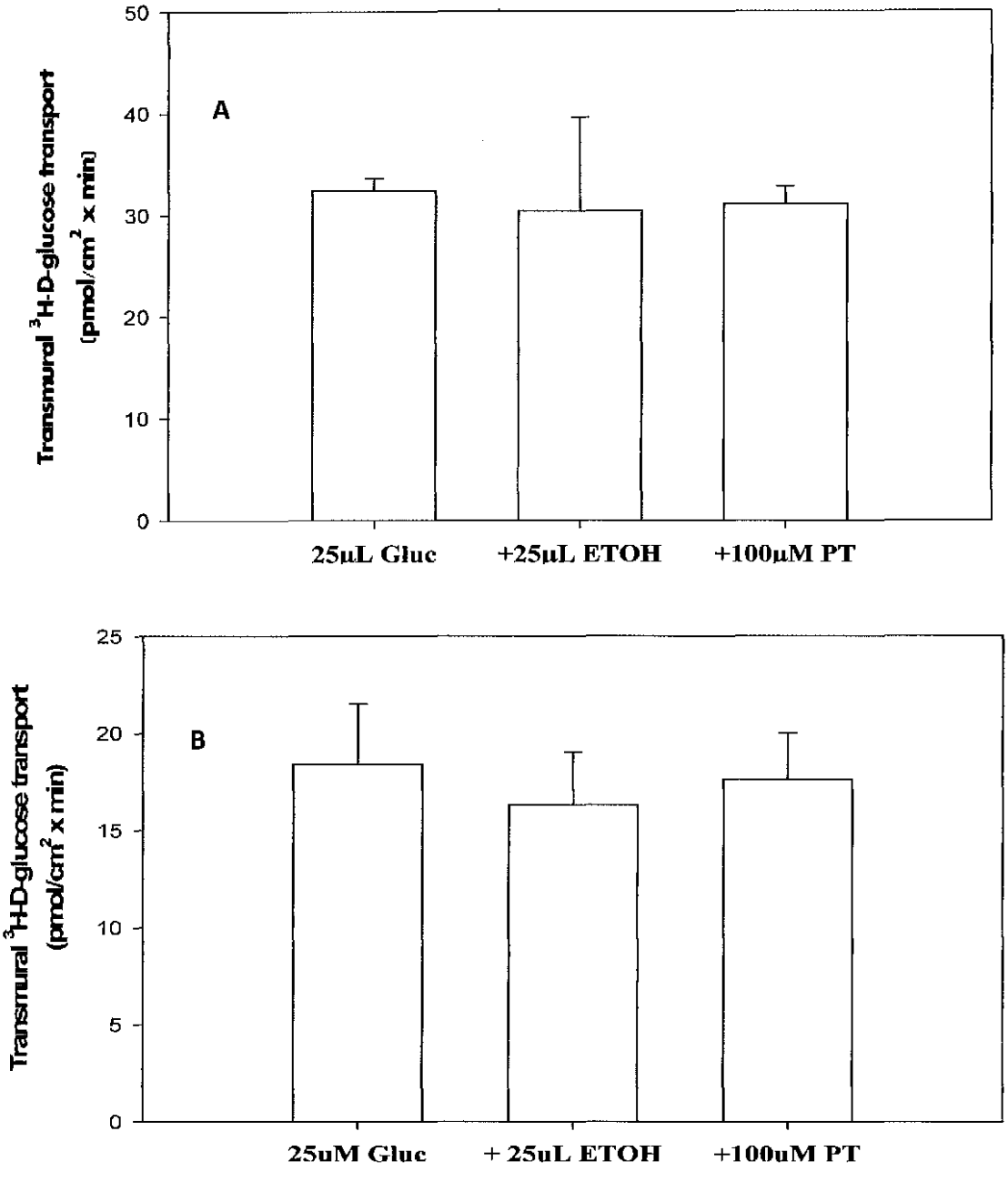

Figure 12: Effect of mucosal 100µM phloretin on 25µM MS ^{3}H-D-glucose transport. Bar graphs are the slopes ± 1 SEM of triplicate replicates at each time point obtained from the time course data. Panels A and B are results obtained from different experiments using individual animals. Phloretin was dissolved in ETOH before adding to incubation medium.

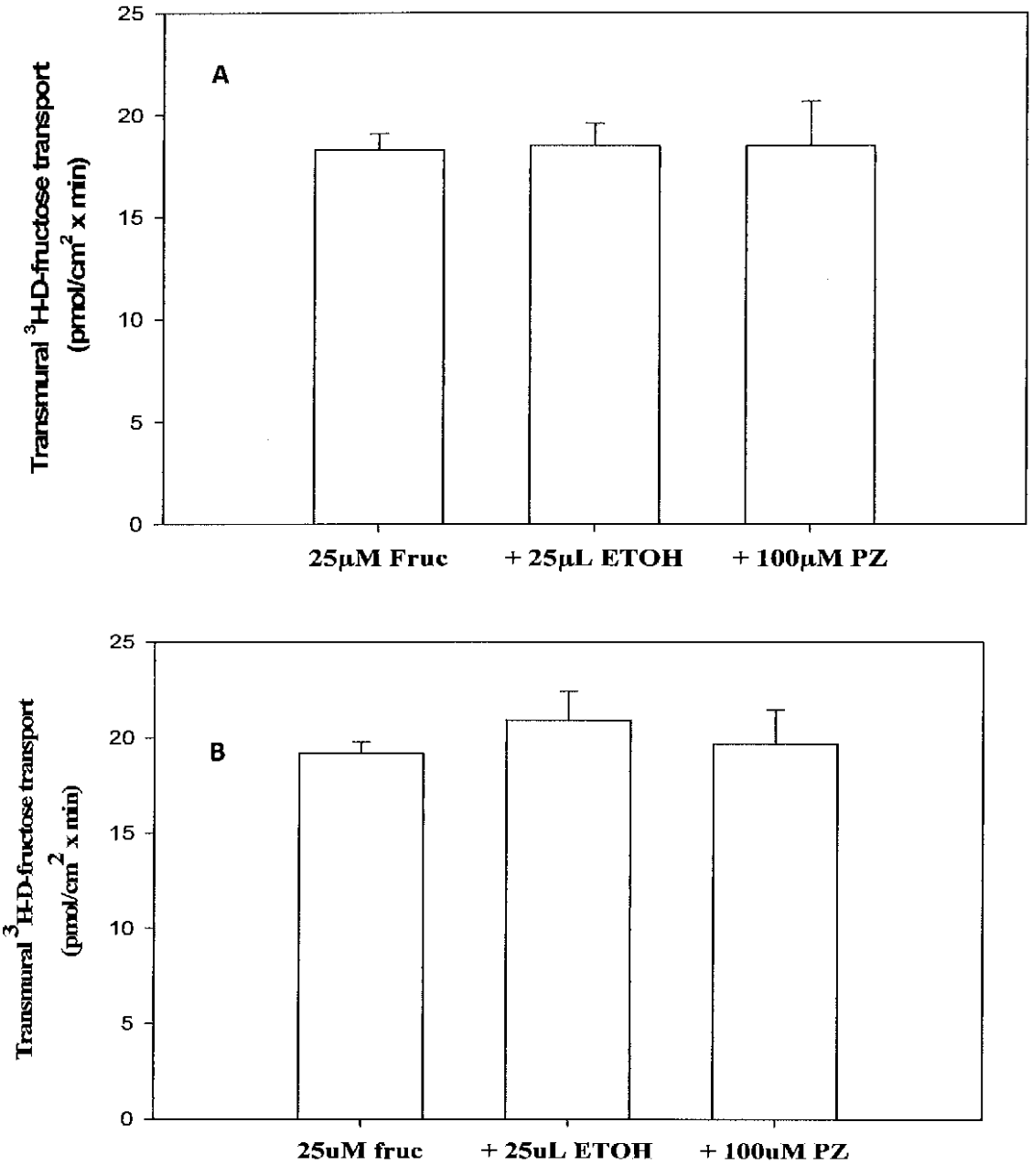

Figure 13: Effect of mucosal 100μM phloridzin on 25μM MS ^{3}H-D-fructose transport. Bar graphs are the slopes ± 1 SEM of triplicate replicates at each time point obtained from the time course data. Panels A and B are results obtained from different experiments using individual animals. Phloridzin was dissolved in ETOH before adding to incubation medium.

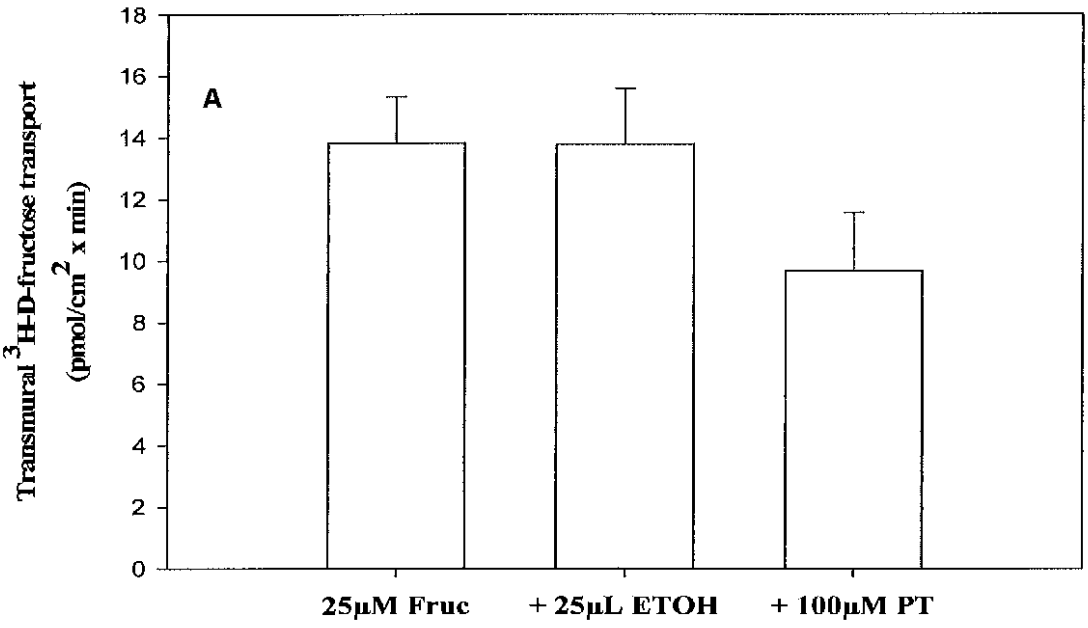

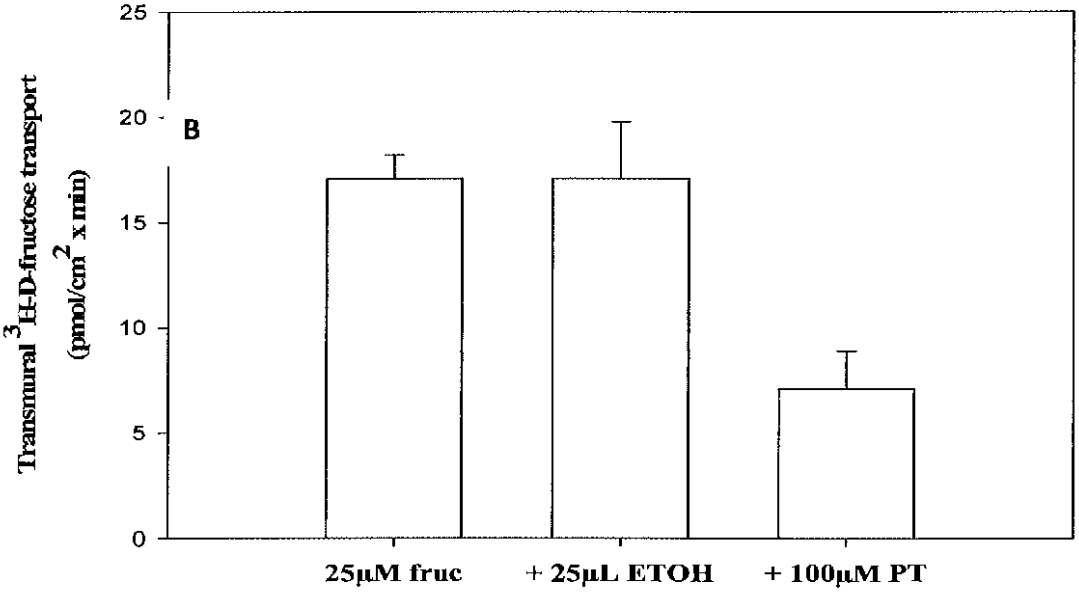

Figure 14: Effect of mucosal 100μM phloretin on 25μM MS ^{3}H-D-fructose transport. Bar graphs are the slopes ± 1 SEM of triplicate replicates at each time point obtained from the time course data. Panels A and B are results obtained from different experiments using individual animals. Phloretin was dissolved in ETOH before adding to incubation medium.

Effect of Varying Concentrations of Mucosal D-glucose on Transmural MS ^{3}H-D-fructose Transport and Varying Concentration of Mucosal D-fructose on Transmural MS ^{3}H-D-glucose Transport.

The effect of increasing mucosal D-fructose (0, 10, 25, 50, 100, and 250μM) on transmural ^{3}H-D-glucose transport is shown in Figs. 15 and 16. The thirty minutes time course uptake of mucosal 5μM ^{3}H-D-glucose transport in the absence of mucosal D-fructose served as the control (Fig. 15). The control represents ^{3}H-D-glucose transport in the absence of fructose. At 10 and 25μM concentrations of mucosal D-fructose, transmural 5μM ^{3}H-D-glucose transport was no different from that of the control (Fig. 15). At 50, 100 and 250μM mucosal D-fructose, 5μM transmural ^{3}H-D-glucose transport was reduced compared to the control (Fig. 15). Similarly, at 10 and 50μM mucosal D-fructose did not affect transmural transport of 25μM ^{3}H-D-glucose (Fig. 16). But transmural 25μM ^{3}H-D-glucose transport was reduced at 100 and 250μM compared to the control (Fig. 16). The effects of increasing mucosal D-glucose on ^{3}H-D-fructose transport are shown in Figs. 17 and 18. Unlike mucosal ^{3}H-D-glucose transport, 5μM ^{3}H-D-fructose transport (Fig. 17) and 25μM ^{3}H-D-fructose transport (Fig. 18) were not decreased at any concentration of mucosal D-glucose compared to the control. These data suggest the presence of a possible shared transport protein located on the serosal intestinal surface that has a higher affinity for D-fructose than for D-glucose.

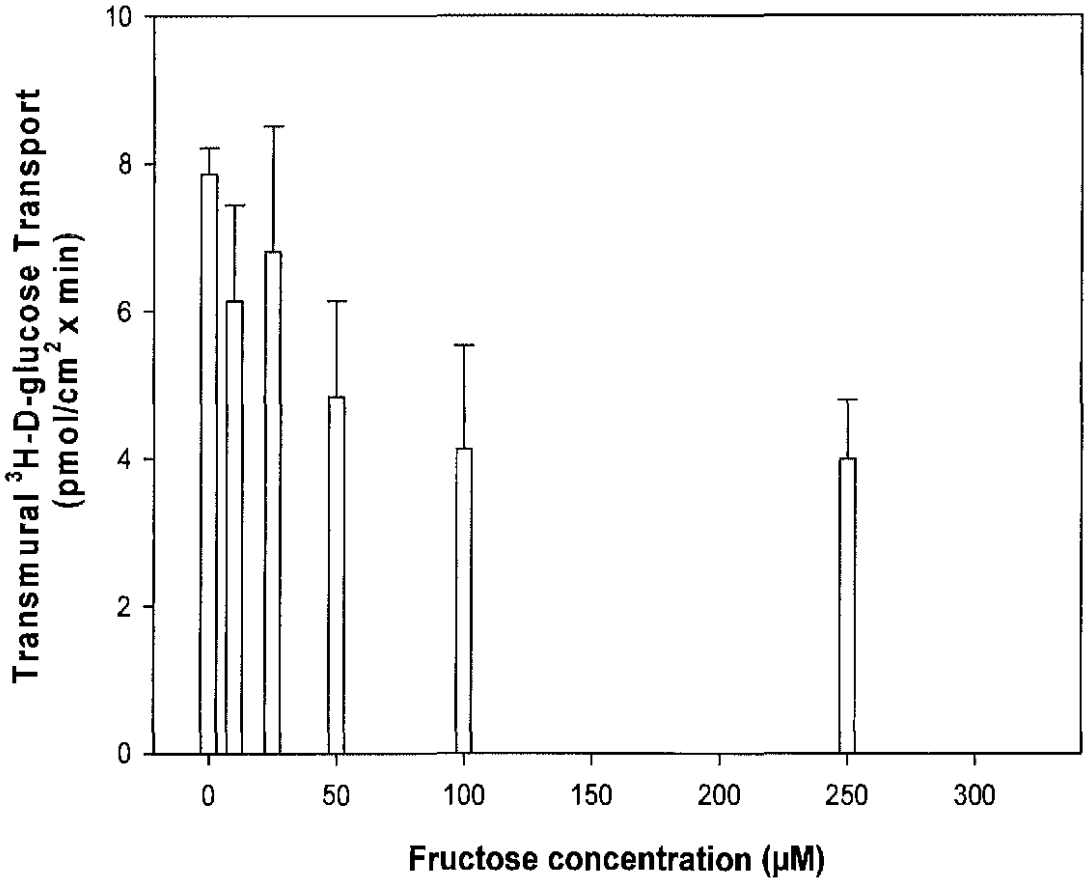

Figure 15: Effect of mucosal D-fructose (0, 10, 25, 50, 100, and 250µM) on MS 5µM ^{3}H-D-glucose transport. Bar graphs are the means ± 1 SEM of triplicate replicates at each time point obtained from the time course data.

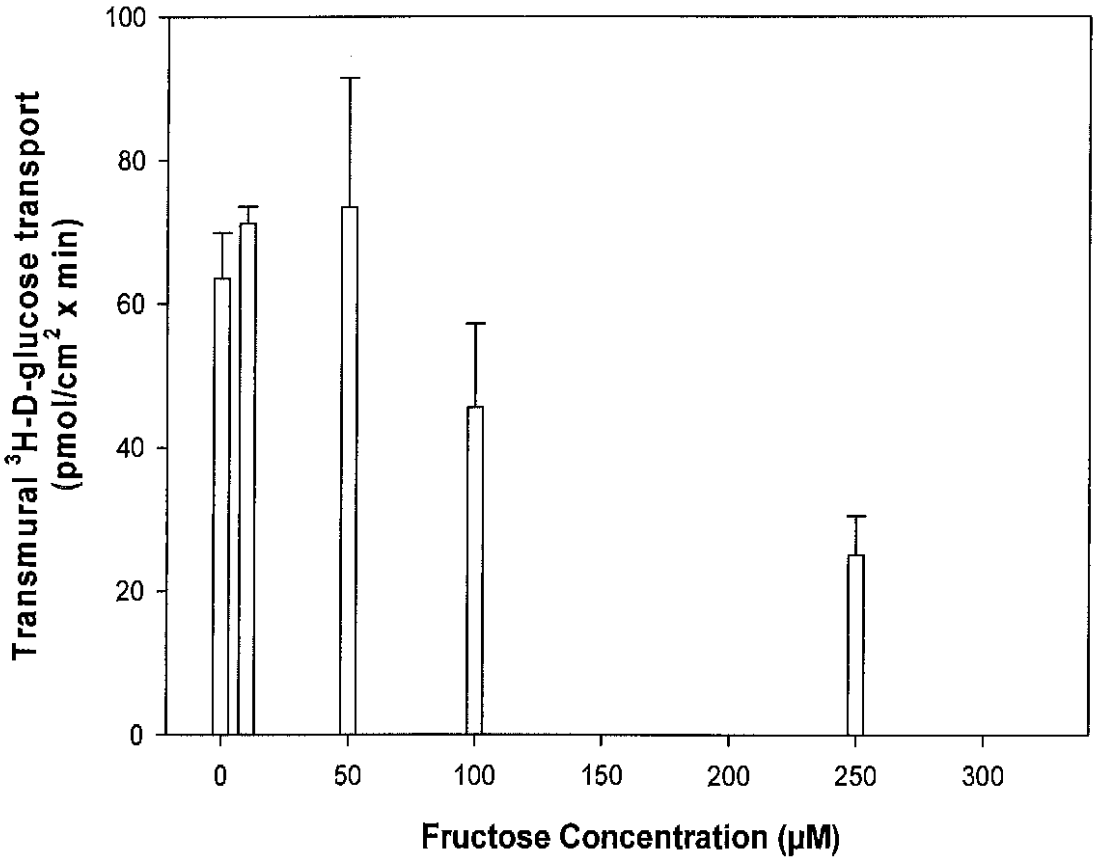

Figure 16: Effect of mucosal D-fructose (0, 10, 25, 50, 100 and 250µM) on MS 25µM ^{3}H-D-glucose transport. Bar graphs are the means ± 1 SEM of triplicate replicates at each time point obtained from the time course data.

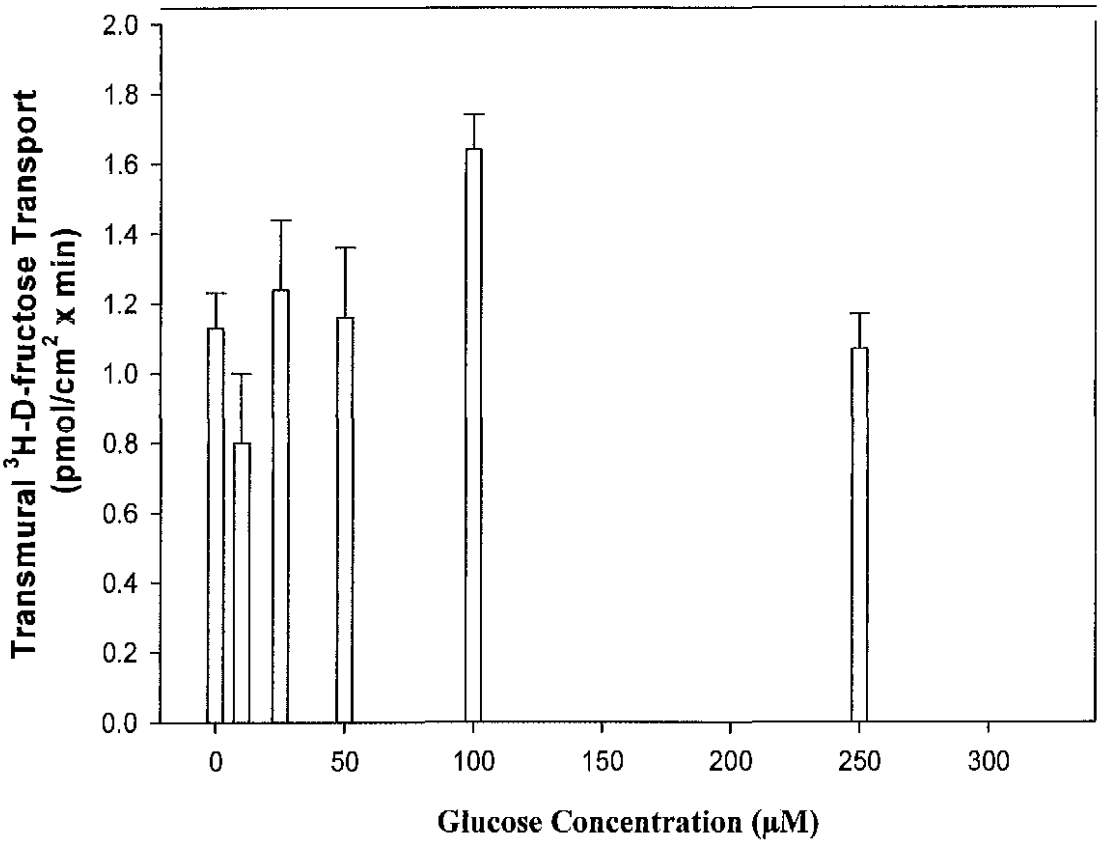

Figure 17: Effect of mucosal D-glucose (0, 10, 25, 50, 100, and 250µM) on MS 5µM ^{3}H-D-fructose transport. Bar graphs are the means ± 1 SEM of triplicate replicates at each time point obtained from the time course data.

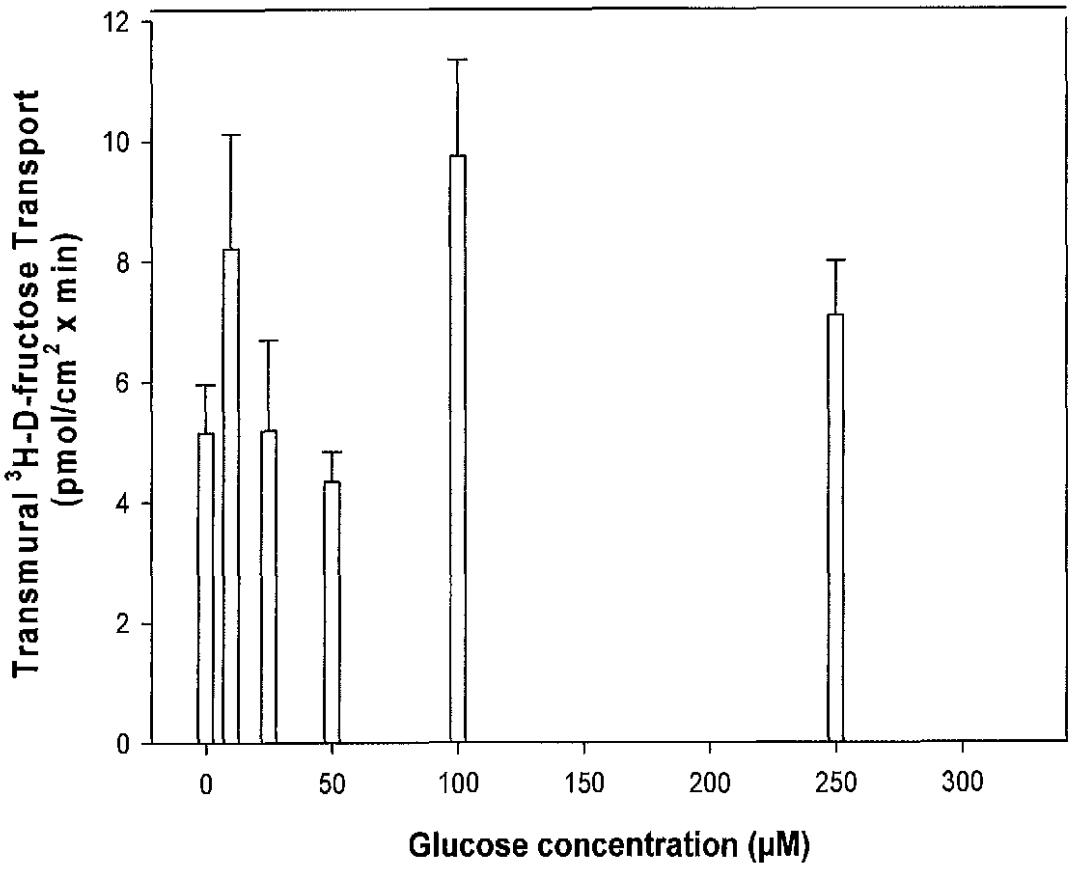

Figure 18: Effect of mucosal D-glucose (0, 10, 25, 50, 100 and 250µM) on MS 25µM ^{3}H-D-fructose transport. Bar graphs are the means ± 1 SEM of triplicate replicates at each time point obtained from the time course data.

Histological Stain and Immunohistochemistry

Histological analysis of the lobster intestine stained with Masson trichrome is shown in Fig. 19A. In this figure, there appear to be projections into the lumen that are somewhat similar to villi. True villi have blood vessels running through the length of the intestinal villi. Blood vessels were not observed in the lobster intestinal villi (Fig. 19A and 19B). These villi-like projections (**V**) are made up of cells that might be responsible for absorption of nutrients. Below the projections are connective tissues (**CT**) and muscles which provide structural support and motility and mediates exchange of nutrients between tissues. In addition, connective tissues and muscles also contain blood cells (**BC**) that are involved in immune defense. A higher magnification of these villi-like projections is shown in Fig. 19B and there appear to be cellular structures that might be responsible for transport of substrates into the cells.

Immunohistochemistry analysis was performed on cross sections of the intestinal tissue to identify the presence of GLUT 5 transport protein responsible for transepithelial mucosal transport of ^{3}H-D-fructose across the intestine (Fig. 20A and 20B). The negative control of the tissue was not incubated in primary antibody (Fig. 20A). The negative control revealed the absence of fluorescence on the villi-like projections. Analysis of the villi-like projections incubated in both primary and secondary antibody is shown in Fig. 20B. The mucosal aspect (**mV**) of the projections showed a greater intensity of green fluorescence than the serosal aspect (**sV**) of the projections (Fig. 20B). Upon analysis, there was a significant difference between the intensity of fluorescence on the mucosal (81.0 ± 3.3) and serosal (35.4 ± 0.9) aspects of the villi-like projections ($P < 0.01$)

suggesting that a GLUT 5-like protein is located on the mucosal membrane of the projections.

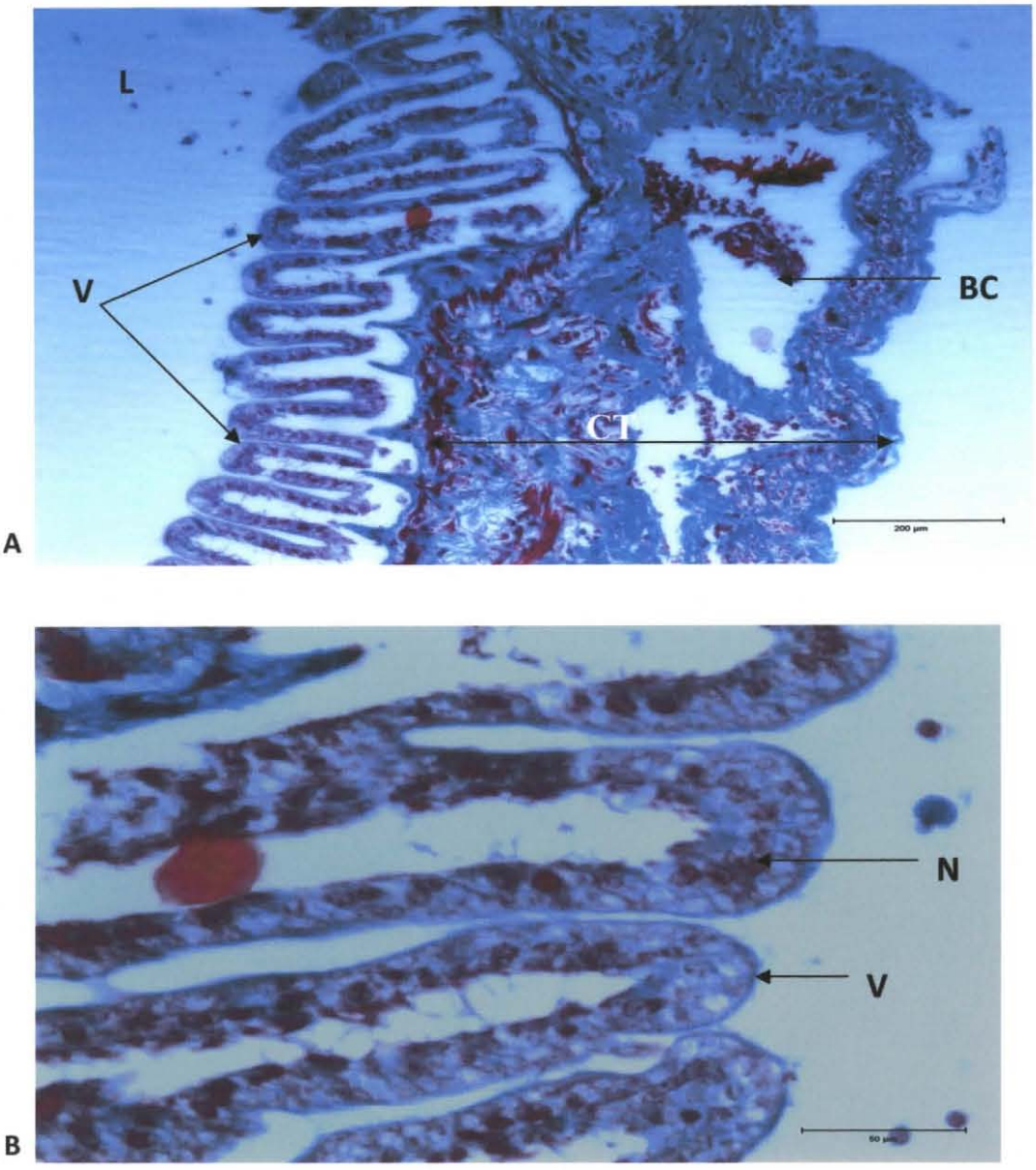

Figure 19: Cross sections of the lobster intestine stained with Masson Trichrome. Tissue sections were fixed in formalin and cut in sections using a microtome. Tissues were visualized using an Olympus BX60 microscope. Structures identified are lumen **L**, Villi-like projections **V**, connective tissues **CT,** and Blood cells **BC**. Magnification bar represents 200µm and 50µm for picture A and B respectively.

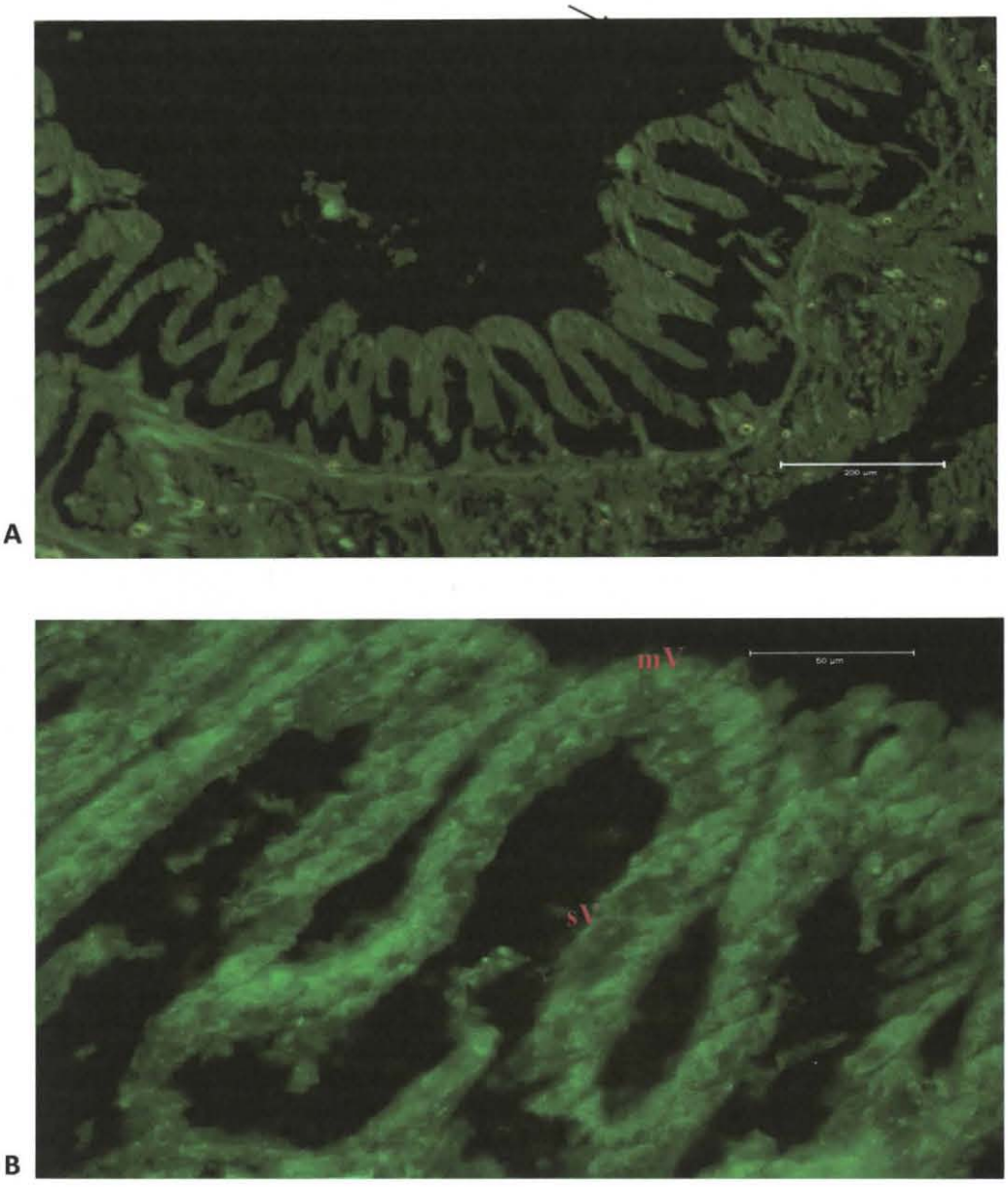

Figure 20: Immunohistochemistry analysis of the lobster intestine. Picture A represents a negative control incubated only in secondary antibody. Picture B represents the experimental treatment incubated in both primary and secondary antibody. Note the increased intensity of fluorescence on the mucosal villi (**mV**) than on the serosal villi, (**sV**). The intensity of fluorescence on **mV** is significantly different from that on **sV** ($P < 0.01$). Magnification bar represents 200μm and 50μm for picture A and B respectively.

Transepithelial Serosal to Mucosal Transport of ^{3}H-D-glucose and ^{3}H-D-fructose

In order to determine the presence of a serosal transporter used by D-glucose and D-fructose, 25μM transepithelial SM ^{3}H-D-glucose transport was investigated in the presence of 100μM serosal fructose (Fig. 21). The same study was conducted on 25μM transepithelial SM ^{3}H-D-fructose transport in the presence of 100μM serosal glucose as well (Fig. 22). Upon analysis, it was determined that 100μM serosal fructose decreased serosal ^{3}H-D-glucose transport by 24% (Fig. 21) while 100μM serosal glucose decreased serosal ^{3}H-D-fructose transport by 14% (Fig. 22). Next, ^{3}H-D-glucose transport was analyzed in the presence of increasing serosal D-glucose concentrations (1, 2.5, 5, 10, 25, 50, and 100μM) (Fig. 23). Curve fitting analysis was achieved using an exponential decay curve with an asymptote: $J_{substrate} = Y_0 + a*\exp(-b* x)$. It was determined that increasing unlabelled serosal D-glucose decreased SM ^{3}H-D-glucose transport and that about 44% of SM ^{3}H-D-glucose transport was carrier mediated (Fig. 23). ^{3}H-D-fructose was analyzed in like manner (Fig. 24). Data analysis revealed that increasing unlabelled serosal D-fructose decreased SM ^{3}H-D-fructose transport by 57% (Fig. 24). The proportion of total SM transport inhibited by the addition of unlabelled substrate was attributed to carrier transport.

To determine whether GLUT 2 is the transport protein responsible for SM ^{3}H-D-glucose and ^{3}H-D-fructose transport, transepithelial SM ^{3}H-D-glucose and ^{3}H-D-fructose transports were investigated in the presence of varying concentrations of serosal phloretin as described above Fig. 25 and 26 respectively. The exponential decay data analysis indicated that while 48% of the initial SM transport of ^{3}H-D-glucose occurred through a

phloretin sensitive transporter (Fig. 24), 54% of the initial SM transport of ^{3}H-D-fructose occurred through a phloretin sensitive transporter (Fig. 26). Thus, these data suggest that a GLUT 2 transport protein is located on the serosal membrane of the intestine and is responsible for SM carrier transport of D-glucose and D-fructose.

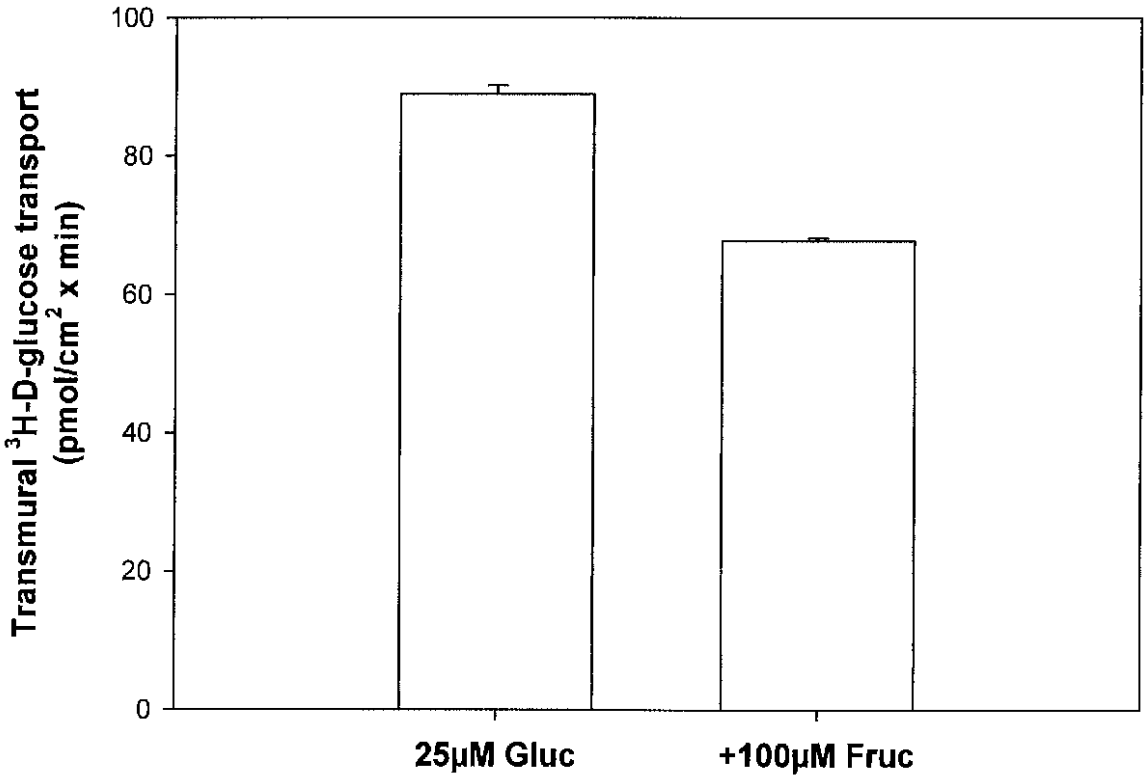

Figure 21: Effect of serosal 100µM D-fructose on 25µM SM transport of ^{3}H-D-glucose. Bar graphs are the means ± 1 SEM of triplicate replicates at each time point obtained from the time course data.

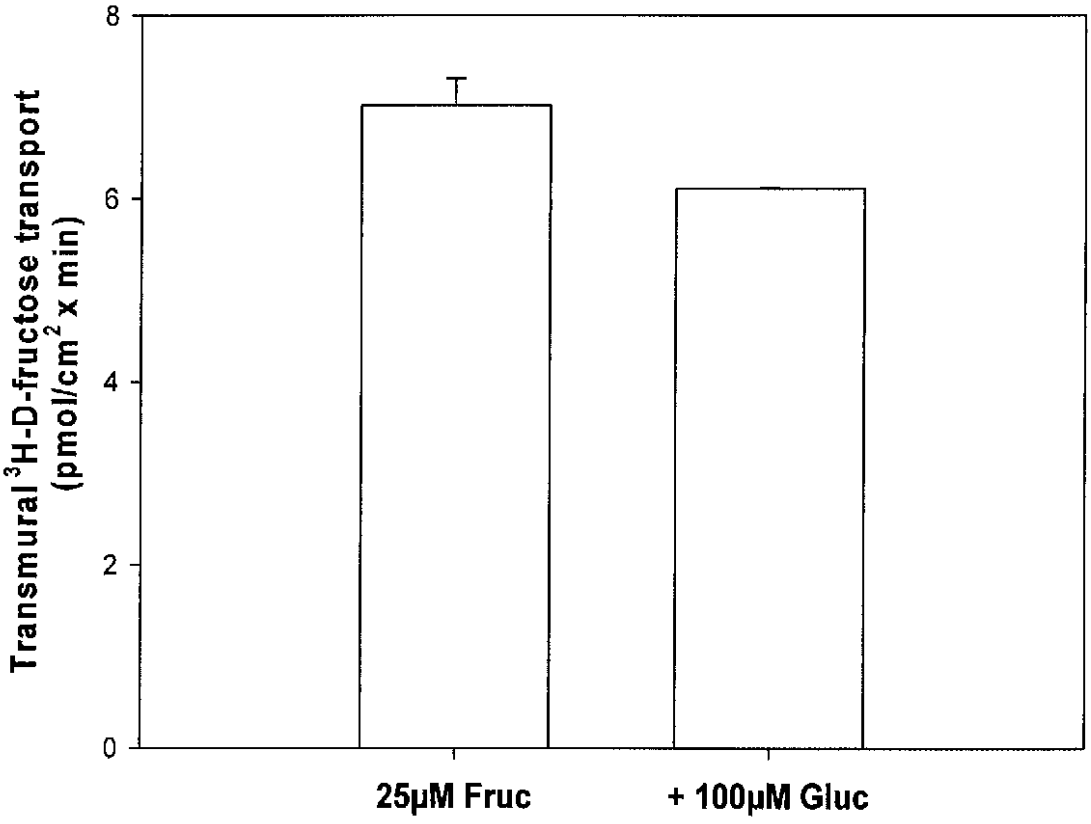

Figure 22: Effect of serosal 100μM D-glucose on 25μM SM transport of ^{3}H-D-fructose. Bar graphs are the means ± 1 SEM of triplicate replicates at each time point obtained from the time course data.

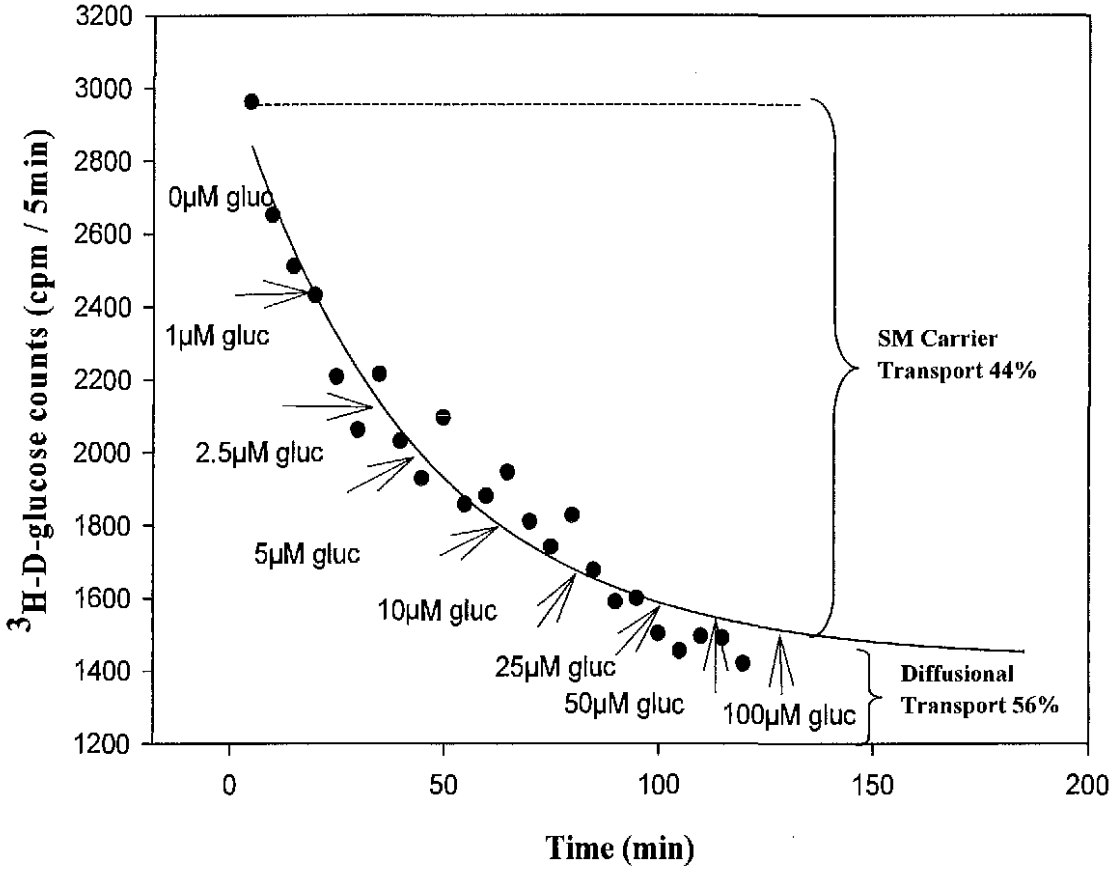

Figure 23: Effect of increasing serosal D-glucose on SM transport of ^{3}H-D-glucose. Symbols are total luminal ^{3}H-D-glucose CPM collected over a 5 min sampling interval at each serosal concentration of glucose. Each arrow on the graph represents the time at which the different concentrations of serosal glucose was added.

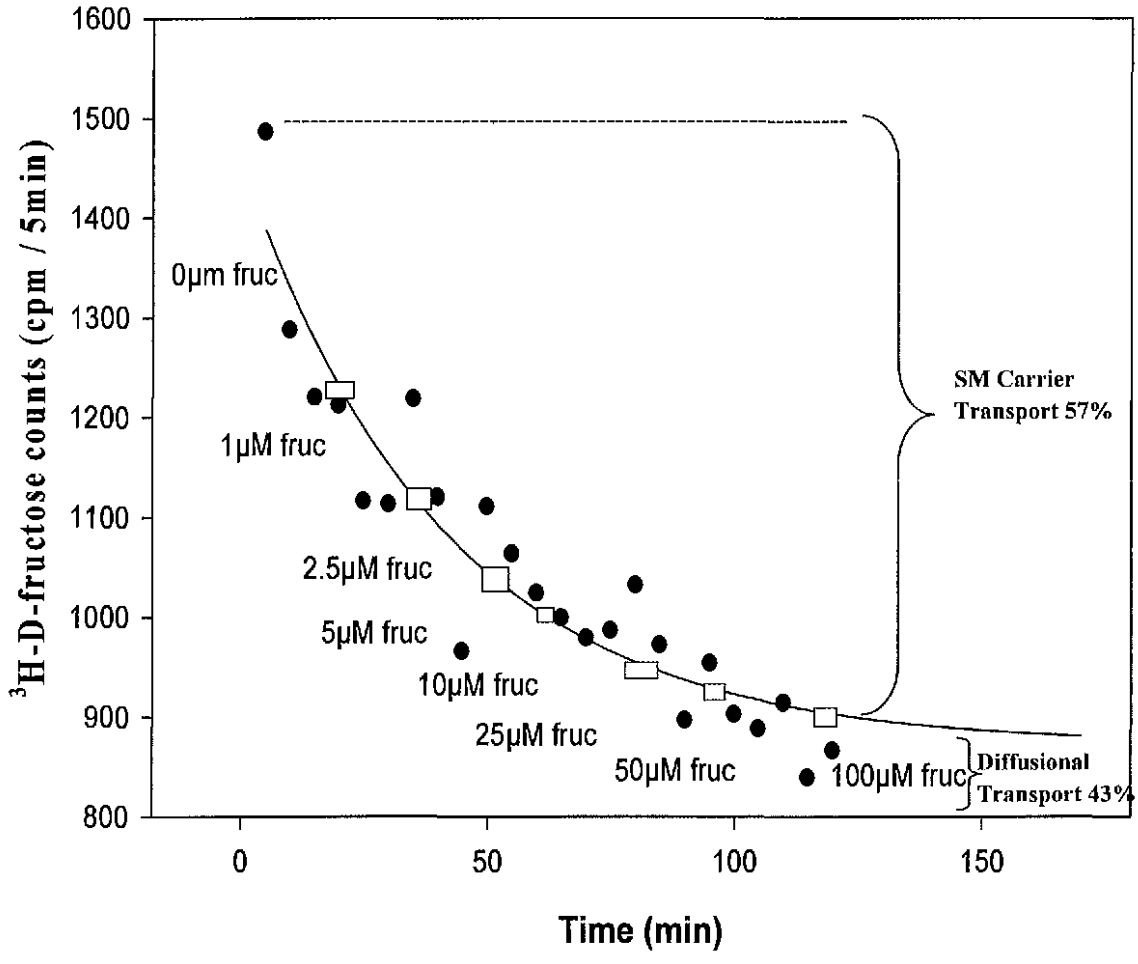

Figure 24: Effect of increasing serosal D-fructose on SM transport of ^{3}H-D-fructose. Symbols are total luminal ^{3}H-D-fructose CPM collected over a 5 min sampling interval at each serosal concentration of fructose. Each box on the graph represents the time at which the different concentrations of serosal fructose was added.

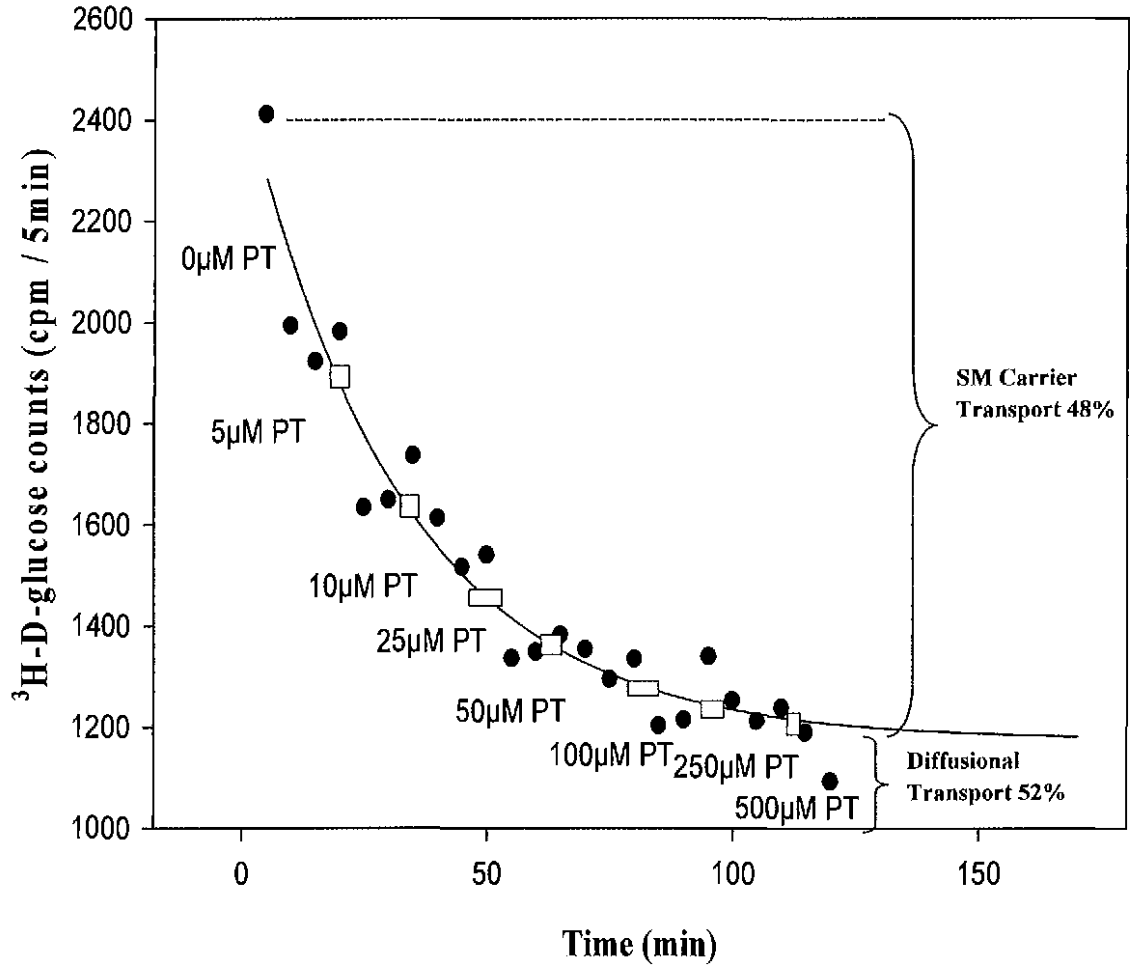

Figure 25: Effect of increasing serosal phloretin on SM transport of ^{3}H-D-glucose. Symbols are total luminal ^{3}H-D-glucose CPM collected over a 5 min sampling interval at each serosal concentration of phloretin. Each box on the graph represents the time at which the different concentrations of serosal phloretin was added.

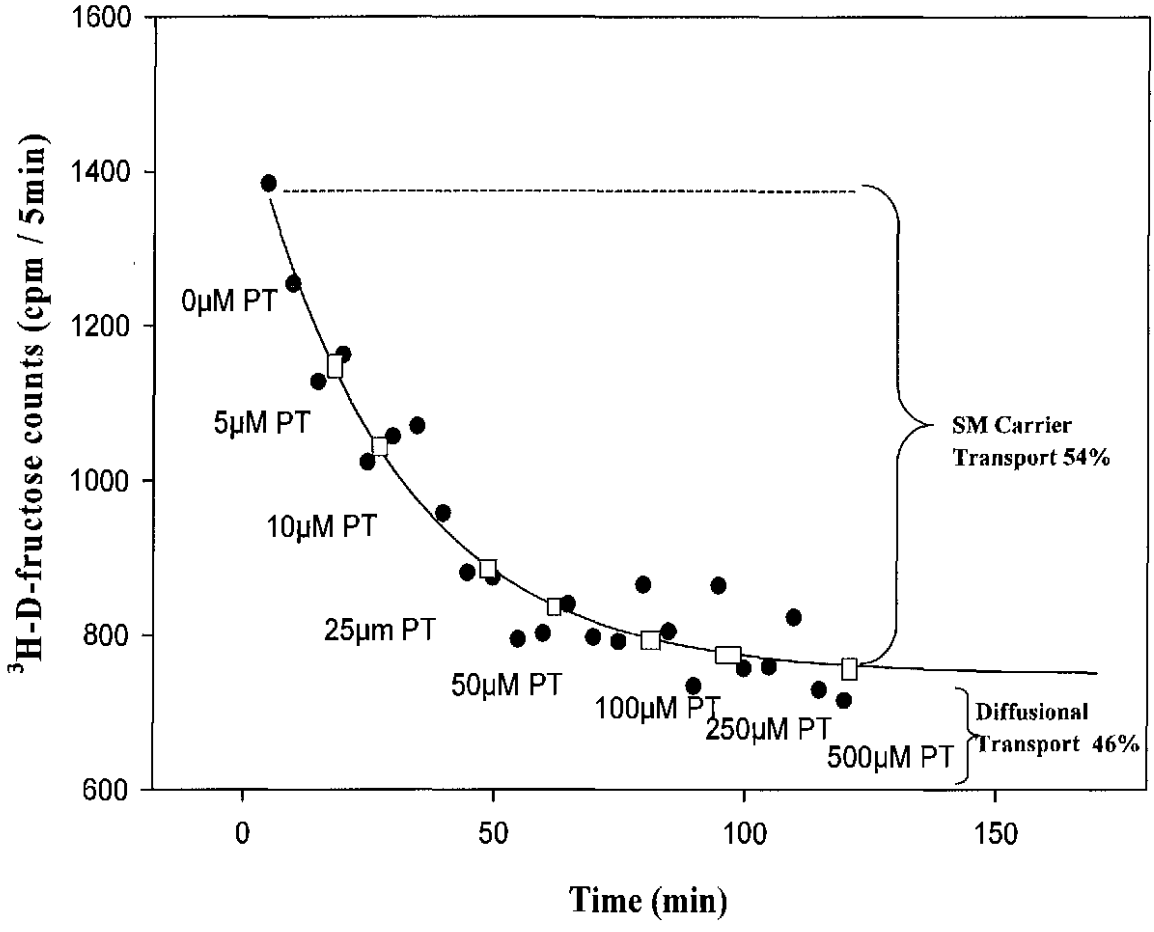

Figure 26: Effect of increasing serosal phloretin on SM transport of ^{3}H-D-fructose. Symbols are total luminal ^{3}H-D-fructose CPM collected over a 5 min sampling interval at each serosal concentration of phloretin. Each box on the graph represents the time at which the different concentrations of serosal phloretin was added.

DISCUSSION

The finding of a homology between mammalian, bacteria and parasitic protozoan sugar transport proteins and the position of crustaceans on the phylogenetic tree between bacteria and mammals is what led to this study. This study was conducted by investigating the absorption of ^{3}H-D-glucose and ^{3}H-D-fructose in physiological saline that mimics the ionic composition of the lobster hemolymph in the presence of varying experimental treatments. The results of the dietary glucose and fructose transport obtained from this present investigation revealed that there has been an evolutionary conservation of function of the sugar transport proteins despite varying environmental and nutritional requirements among these organisms over time.

^{3}H-D-glucose and ^{3}H-D-fructose Transport Kinetics

In order to determine the presence of mucosal and serosal D-glucose and D-fructose transport proteins, experiments were conducted that involved increasing mucosal and serosal D-glucose and D-fructose concentrations and measuring the sugar transport rates across the intestine at each concentration. These transport rates were found to be hyperbolic functions (Figs. 7 and 10). The hyperbolic curves followed the Michaelis-Menten equation:

$$V = \frac{J_{max}\,[S]}{(K_m + [S])}$$

Where J_{max} is the maximum transport velocity, K_m is the concentration at half maximal transport velocity, S is substrate concentration and V is the rate of the reaction. The findings of hyperbolic transport functions suggest that both MS and SM D-glucose

transport are mediated by transport proteins. The kinetic constants of MS and SM D-glucose transport are shown in Table 1. The K_m constant indicates that at that concentration of MS or SM D-glucose, the transport protein is half saturated and is therefore working at half the maximum speed. The values of the J_{max} of MS or SM D-glucose transport indicate the maximum transport rate of MS and SM D-glucose transport. This means that any concentration of mucosal or serosal D-glucose above its maximum transport rate will not change the rate of its uptake. Intestinal net fluxes of D-glucose and D-fructose as indicated in Figs. 7 and 10 does suggest that there is a net absorption of both sugars across the intestine. It was noted earlier that the crustacean intestine is considered a scavenger organ that is responsible for absorbing excess dietary sugars that were not otherwise absorbed by the hepatopancreas; as a result, the transport proteins located on the intestine should have a higher affinity for the uptake of both sugars than in the hepatopancreas. This point is supported by comparing the kinetic constants of both sugars in the hepatopancreas and in the intestine. The K_m for both D-glucose and D-fructose in the hepatopancreas is in the mM range (Verri et al., 2001) in comparison to the μM range in the intestine (Table 1) supporting a higher affinity binding proteins for both sugars. It is also important to note that the maximum transmural MS flux of D-glucose was 4 times that of SM D-glucose flux (Table 1) and supports a net absorption of D-glucose across the intestine.

Although MS and SM ^{3}H-D-fructose influx kinetic curves show hyperbolic functions (Fig. 10), the MS and SM transport rates of ^{3}H-D-fructose were much lower than MS and SM D-glucose transport rates (Fig. 7 and 10). The lower kinetic constants for SM D-fructose transport than SM D-glucose transport suggest a much higher affinity

transport protein for fructose than glucose on the serosal membrane of the intestine (Table 1). A comparison of MS kinetic constants, K_m values, for fructose in the hepatopancreas and in the intestine also reveals a higher affinity transport protein for fructose in the intestine (Table 1) than in the hepatopancreas (Sterling et al., 2009). Similar to glucose transport, there was a net absorption of dietary fructose across the intestine but the maximum transport rate, J_{max} of MS D-fructose transport, was only twice that of the SM transport of D-fructose (Table 1). Lastly, the maximum transport of MS D-glucose was 10 times greater than MS D-fructose maximum transport rate, while SM D-glucose maximum transport rate was only about 4 times SM D-fructose transport rate. These kinetics data lead to the following conclusions: (1) The presence of D-glucose and D-fructose transport proteins, (2) A net absorption of D-glucose and D-fructose, (3) Higher affinity fructose transporters than glucose transporters and (4) Higher affinity transporters for both sugars in the intestine than in the hepatopancreas.

Effect of phloridzin and phloretin on MS ^{3}H-D-glucose and ^{3}H-D-fructose Transport

Several inhibitors like phloridzin and phloretin are known to affect the sodium dependent glucose transporter and the facilitated sugar transporters. Shapiro (1946) demonstrated that phloridzin prevents glucose reabsorption by interfering with phosphorylation of glucose. Phloretin on the other hand interferes with transport of sugars by interfering with the orientation and conformation of the sugar molecules (Andersen et al., 1976). In studies performed on other organisms, there was molecular evidence that the mammalian gene sequences of sugar transporters were similar to sugar transport gene sequences in bacteria (Maiden et al., 1987) and in lobster (Sterling et al.,

2009). In this study, phloridzin was used to characterize mucosal sodium dependent D-glucose transport, while phloretin was used to characterize the possible presence of facilitated glucose transporter, GLUT 2, on both the mucosal and serosal intestinal surfaces. Treatment of 100μM phloridzin decreased mucosal 25μM D-glucose transport compared to the control (Fig. 11). Since phloridzin was dissolved in 100% ethanol, transport of 25μM D-glucose was studied in the presence of 100% ethanol and the data showed that there was no significant difference in D-glucose transport in the presence of 100% ethanol (Fig. 11). Conversely, 100μM phloridzin did not inhibit 25μM ^{3}H-D-fructose transport compared to the control (Fig. 13). These findings suggest that the SGLT 1 transport protein is present on the mucosal membrane of the intestine and it is responsible for mucosal D-glucose transport but not for D-fructose transport.

The above findings of an SGLT 1 transport protein are similar to the mechanism of mucosal transport of D-glucose and D-fructose found in other organisms. In mammals, SGLT 1 is located on the human chromosome 23 (Wright et al., 2004) and is found on the apical membrane of the absorptive intestinal cells (Wood and Trayhurn. 2003). Homologues of the SGLT gene family are found in yeast, insects and bacteria (Turk and Wright. 1997). Characterization of a sodium/glucose cotransporter revealed the presence of an SGLT 1 homologue in bacteria, *Vibro parahaemolyticus* (Xie et al., 2000), insects, *Aphidius ervi* (caccia et al., 2007), and in the hepatopancreas of the American lobster, *Homarus americanus* (Sterling et al., 2009). For D-fructose transport, there is no evidence that D-fructose transport is sensitive to phloridzin but recently, there was evidence that D-fructose might be absorbed in the hepatopancrease through a different

sodium dependent transporter, SGLT 4 (Sterling et al., 2009) which was first identified in humans (Tazawa et al., 2005).

In Fig. 12, ^{3}H-D-glucose transport was insensitive to treatment of 100μM phloretin, but not with ^{3}H-D-fructose transport which showed a 30 to 58 percent decrease in the transport rate (Fig. 14). The lack of sensitivity of ^{3}H-D-glucose to phloretin could be explained by the low affinity binding of D-glucose to GLUT 2 (Wood and Trayhurn. 2003). Since ^{3}H-D- glucose has a low binding affinity to GLUT 2, treatment of phloretin will not decrease ^{3}H-D-glucose transport (Fig. 12) because of the presence of SGLT 1 transport protein which is specific for mucosal transport of ^{3}H-D-glucose. On the contrary, because of the high affinity binding of ^{3}H-D-fructose to GLUT 2, treatment of phloretin decreased ^{3}H-D-fructose transport (Fig. 14). In a study conducted by Caccia et al., (2007), the data revealed the absence of a GLUT 2 on the midgut of the insect, *Aphidius ervi* at low glucose levels. At very high glucose levels, the study revealed that GLUT 2 was rapidly inserted on the mucosal membrane for absorption of excess glucose. The finding of GLUT 2 on the mucosal membrane of the lobster intestine at a low sugar concentration, as shown in Fig. 14, revealed not only a difference between sugar transport in the lobster intestine and in the midgut of an insect (Caccia et al., 2007), but also a difference between the lobster intestine and mammals (AU et al., 2002). Furthermore, there was evidence in previous studies of a facilitated D-fructose transporter, GLUT 5, on the intestinal mucosal membrane (Miyamoto et al., 1994). In intact mammalian intestine, GLUT 5 is highly specific for fructose (Miyamoto et al., 1994; Kellet, 2001).

In previous studies, molecular analysis had been used to determine the presence of a GLUT 5 transport protein on cellular membranes. In this study, immunohistochemistry was used to determine the presence of the GLUT 5 transport protein on the intestinal mucosal membrane (Fig. 20A and 20B). Prior to immunohistochemistry analysis, cross sections of the lobster intestine were histologically fixed and prepared in paraffin. Observations of the slides revealed the presence of projections that looked like villi (Fig. 19A). Under a higher magnification, the projections seemed to have cellular structures that might be responsible for absorption of nutrients (Fig. 19B). When sections were incubated in both primary and secondary antibodies, there was an indication of a greater intensity of fluorescence on the mucosal aspect of the intestinal projections compared to the serosal aspect (Fig. 20B). This result suggests the presence of a GLUT 5 transporter on the mucosal membrane of the intestine as previously observed in other studies (Caccia et al., 2007; Corpe et al., 2002; and Miyamoto et al., 1994).

Transepithelial Serosal to Mucosal Transport of D-glucose and D-fructose

Evidence for the presence of a serosal transport protein for glucose and fructose transport is supported by Fig. 21, 22, 23 and 24. In Fig. 23, increasing serosal D-glucose concentration resulted in a 44% decrease in the SM transport of ^{3}H-D-glucose. The same effect was observed in the SM transport ^{3}H-D-fructose when serosal D-fructose was increased; SM transport of ^{3}H-D-fructose was decreased by 57% (Fig. 24). GLUT 2 was determined to be present on the serosal membrane as observed by decrease in the SM transport of ^{3}H-D-glucose and SM transport of ^{3}H-D-fructose upon increasing the

concentration of serosal phloretin (Fig. 25 and 26), respectively. The observation of a shared GLUT 2 transport protein by D-glucose and D-fructose on the serosal membrane has been previously reported in mammals (Drozdowski and Thomson, 2006), and in insects (Caccia et al., 2007).

Increasing mucosal fructose decreased 5μM ^{3}H-D-glucose transport at 50, 100 and 250μM concentrations while at 25μM ^{3}H-D-glucose concentration, ^{3}H-D-glucose was only decreased at 100 and 250μM concentration of D-fructose (Fig. 13 and 14) respectively. Conversely, both 5μM and 25μM ^{3}H-D-fructose transport was not decreased at any concentration of mucosal D-glucose compared to the control (Fig. 15 and 16). A possible explanation for the observed inhibition of ^{3}H-D-glucose by mucosal D-fructose is that since both sugars share the same exit transport protein, GLUT 2, on the serosal membrane, and D-fructose has a higher binding affinity for GLUT 2, and increasing mucosal D-fructose will inhibit the exit transport of ^{3}H-D-glucose. In other words, because D-fructose will more readily bind GLUT 2, increasing mucosal D-fructose concentration will out compete ^{3}H-D-glucose binding to GLUT 2, thereby inhibiting ^{3}H-D-glucose exit from the cell. The lack of inhibition of ^{3}H-D-fructose by D-glucose had been supported in previous studies by Corpe et al., 2002 and Miyamoto et al., 1994.

Woking Model of D-glucose and D-fructose Transport in the Lobster Intestine.

Figure 27 represents the proposed working model for the mechanism of MS and SM D-glucose and D-fructose transport across the American lobster, *Homarus americanus,* intestine. This model is based on the physiological investigations reported in

this study. The presence of a sodium/glucose cotransporter, SGLT 1, on the mucosal membrane is supported in this model in Figure 9. Likewise, the presence of a mucosal GLUT 2 and GLUT 5 transport proteins is supported by Fig. 12 and Fig. 20, respectively. Finally, on the serosal membrane the presence of a GLUT 2 transport protein is supported by data represented in Figure 25 and 26. The Na^+/K^+ ATPase pump supplies Na^+ for cotransport of glucose into the cell. The similarities between the working model for the transport of D-glucose and D-fructose across the lobster intestine and the standard model proposed in mammals (Fig. 3) are the presence of an SGLT1 and GLUT 5 transport proteins on the mucosal membrane and the presence of a shared serosal GLUT 2 transport protein. The only difference between the two models as documented by this study is that in mammals, GLUT 2 is inserted in the presence of a high concentration of sugar unlike in the lobster intestine where GLUT 2 is present at low sugar concentration. The similarities between transepithelial sugar transport mechanisms in the lobster and mammalian intestine suggest a highly conserved sugar transport protein suite for the absorption of D-glucose and D-fructose.

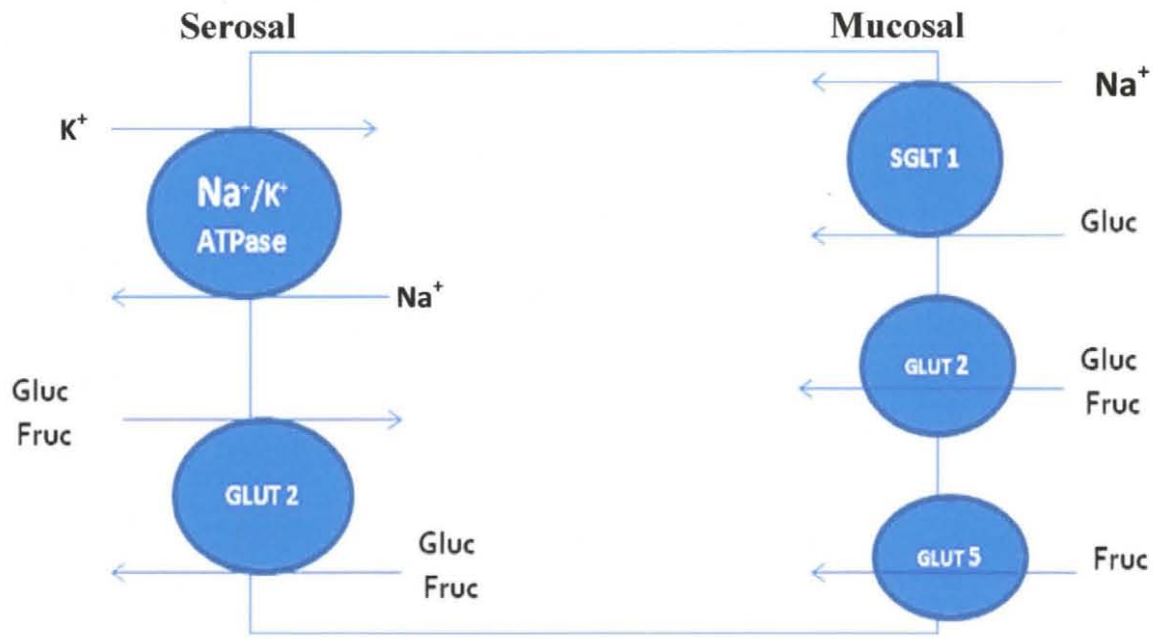

Figure 27: Working model of D-glucose and D-fructose transport across the American lobster, *Homarus americanus*, intestine. The working model is based on the physiological analysis of the mechanism of sugar transport presented in this study and is similar to the proposed standard model of sugar transport in mammals (Kellet, 2001; Manolescu et al., 2007; Miyamoto et al., 1994; Wood and Trayhurn, 2003; and Wright et al., 2007).

CONCLUSION

The following points can be concluded from this study:

1. Transepithelial MS and SM D-glucose and D-fructose transport follows the Michaelis Menton equation indicating the presence of mucosal and serosal transport proteins for D-glucose and D-fructose on the lobster intestinal membrane.

2. Net flux data of MS and SM D-glucose and D-fructose transport indicates a net absorption of D-glucose and D-fructose across the intestinal epithelium.

3. A comparison of kinetic constants of transepithelial SM D-glucose and D-fructose transport suggests a serosal transport protein that has a higher affinity for D-fructose than D-glucose.

4. The effect of phloridzin on mucosal D-glucose and D-fructose transport reveals the presence of a phloridzin-sensitive, SGLT 1-like, transporter on the mucosal membrane responsible for mucosal entry of D-glucose into the cell.

5. GLUT 2 is present on the mucosal membrane of the lobster intestine with a higher binding affinity for D-fructose as observed by the sensitivity of mucosal phloretin to D-fructose but not to D-glucose.

6. Immunohistochemistry analysis shows the presence of a GLUT 5-like transporter on the apical membrane of the intestine and is responsible for mucosal D-fructose transport into the cell.

7. Inhibition studies of the effect of D-glucose on D-fructose transport and D-fructose on D-glucose transport reveals a shared transport protein for both sugars for exit out of the cell.

8. Analysis of the effect of serosal D-glucose inhibiting ^{3}H-D-glucose transport and serosal D-fructose inhibiting ^{3}H-D-fructose suggests that 50 percent of serosal to mucosal transport of both sugars occurs through cellular or paracellular diffusion.

9. The effect of increasing serosal phloretin on D-glucose and D-fructose transport indicates the presence of a carrier mediated GLUT 2-like transport protein utilized by both sugars for exit out of the cell.

WORKS CITED

1. Ahearn, G.A., and Maginniss L.A. (1976) Kinetics of Glucose Transport by the Perfused Mid-Gut of the Freshwater Prawn *Macrobrachium rosenberg II.* J. Physiology 271: 319-336.

2. Andersen, O. S., Finkelstein, A., Katz, I., and Cass A. (1976). Effect of Phloretin on the Permeability of Thin Lipid Membranes. Journal of General Physiology 67: 749-771.

3. AU, A., Gupta, A., Schembri, P., Cheeseman, C.I. (2002) Rapid Insertion of GLUT 2 into the Rat Jejunal Brush-Border Membrane Promoted by Glucagon-like Peptide 2. Biochem. J. 367: 247-254.

4. Caccia, S., Casartelli, A., Losa. E., de Eguileor, M., pennacchio, F., and Giordana, B. (2007) The Unexpected Similarity of Intestinal Sugar Absorption by SGLT 1 and Apical GLUT 2 in an Insect (*Aphidius ervi*, Hymenoptra) and Mammals. Am. J. Physio. 292: R2284-R2291.

5. Corpe, C. P., Bovelander, F. J., Munoz. C. M., Hoekstra, J. H., Simpson, I. A., Kwon, O., Levine, M., Burant, C. F. (2002) Cloning and Functional Characterization of the Mouse Fructose Transporter, GLUT 5. Biochimica et Siophysica Acta. 1576: 191-197

6. Chu, K. H. (1986) Glucose Transport by the in vitro Perfused Midgut of the Blue Crab, *Callinectes sapidus*. J. Exp. Biol. 123: 325-344.

7. Drozdowski, L.A., and Thomson A. B. (2006) Intestinal Sugar Transport. World Journal of Gastroenterology. 12(11): 1657-1670.

8. Henderson, P. J. F. (1990) Proton-Linked Sugar Transport Systems in Bacteria. Bioenergetics and Biomembranes. 22: 525-569.

9. Kellet, G. L. (2001) The Facilitated Component of Intestinal Glucose Absorption. J. Physiol. 531: 585-595.

10. Maiden, M. C. J., Davis, E. O., Baldwin, S. A., Moore, D. C. M., and Henderson, P. J. F. (1987) Mammalian and Bacteria Sugar Transport Proteins are Homologous. Nature. 325: 641-643.

11. Manolescu, A. R., Augustin, R., Moley, K., and Cheeseman, C. (2007) A Highly Conserved Hydrophobic Motif in the Exofacial Vestibule of the Fructose Transporting SLC2A Proteins Acts as a Critical Determinant of their Substrate Selectivity. Mol. Mem. Biol.5-6: 455-463.

12. Manolescu, A. R., Witkowska, K., Kinnaird, A., Cessford, T., and Cheeseman, C. (2007) Facilitated Hexose Transporters: New Perspective on Form and Function. Physiology. 22: 234-240.

13. Manolescu, A., Salas-Burgos, A. M., Fischbarg, J., and Cheeseman, C. I. (2005) Identification of a Hydrophobic Residue as a Key Determinant of Fructose Transport by the Facilitative Hexose Transporter SLC2A (GLUT7). J. Biol. Chem. 280 (52): 42978-42983.

14. Miyamoto, K. I., Tatsumi, S. Morimoto, A., Minami, h., Yamamoto, H., Sone, k., Taketani, Y., Nakabou, Y., Oka, T., Takeda, E. (1994) Characterization of the Rabbit Intestinal Fructose Transporter (GLUT 5). Biochem. J. 303: 877-883.

15. Raven, P. H., Johnson, G. B., Losos, J. B., Mason, K. A., and Singer, S. R. 2008. Biology. New York: McGraw Hill. 1259p.

16. Shapiro, B. (1946). The Mechanism of Phloridzin Glucosuria. Biochem. J. 41(2): 121-154.

17. Sterling, K. M., Cheeseman, C. I, and Ahearn, G. A. (2009) Identification of a Novel Sodium-Dependent Fructose Transport Activity in the Hepatopancreas of the Atlantic Lobster *Homarus americanus*. J. Exp. Biol. 212: 1912-1920.

18. Tazawa, S., Yamato, T., Fujikura, H., Hiratochi, M., Itoh, F., Tomae, M., Takemura, Y. Maruyama, H., Sugiyama, T., Wakamatsu, A., Isogai, T., and Isaji, M. (2005) SLC5A9/SGLT4, a New Na^+-dependent Glucose Transporter, is an Essential Transporter for Mannose, 1,5- anhydro-D-glucitol, and Fructose. Life Sciences 76: 1039-1050.

19. Tetaud, E., Barrett, M. P., Bringaud, F., Baltz, T. (1997) Kinetoplastid Glucose Transporters. Biochem. J. 325: 569-580.

20. Turk, E., Kerner, C. J., Lostaos, M. P., and Wright, E. M. (1996) Membrane Topology of the Human Na^+/Glucose Cotransporter SGLT1. Journal of Biological Chemistry 271 (4): 1925-1934.

21. Turk, E., Wright, E. M. (1997) Membrane Topolpgy Motifs in the SGLT Cotransporter Family. J. Membrane Biol. 159: 1-20.

22. Verri, T., Mandal, A., Zilli L., Bossa, D., Mandal, P.K., Ingrosso, L., Zonno, V., Vilelli, S., Ahearn, G.A., and Storelli, C. (2001) D-Glucose Transport in Decapod Crustacean Hepatopancreas. Comp. Biochem. Physiol. A. 130: 585-606.

23. Walmsley, A. R., Barrett, M. P., Bringaud, F., and Gould, G. W. (1998) Sugar Transporters from Bacteria, parasites and Mammals: Structure-Activity Relationships. TIBS reviews, 23: 476-481.

24. Wood, S., and Trayhurn, P (2003) Glucose Transporters (GLUT and SGLT): Expanded Families of Sugar Transport Proteins. British Journal of Nutrition 89: 3-9.

25. Wright, E.M., Hirayama, B.A., and Loo D.F. (2007) Active Sugar Transport in Health and Disease. J. Internal Med. 261: 32-43.

26. Wright, E. M., Loo, D. D. F., Hirayama, B. A., and Turk, E. (2004) Surprising Versatility of Na+ -Glucose Cotransporters: SLC5. Int. Union Physiol. Sci. 19: 370-376.

27. Wright, S. H. and Ahearn, G. A. (1997) Nutrient Absorption in Invertebrates. IN: Handbook of Physiology (Sect. 13: Comparative Physiology), Vol. II, Chap. 16: 1137-1206.

28. Xie, Z., Turk, E., and Wright, E. M. (2000). Characterization of the vibro parahaemolyticus Na^+/ Glucose Cotransporter. J. Biolo. Chem. 275 (4): 25959-25964.

VITA

Ijeoma Ebelechukwu Obi was born on in . She completed her B.S. in Microbiology in 2006 at the University of Florida in Gainesville, FL. Ijeoma became a graduate student at the University of North Florida in January 2008. As an M.S Biology student, she was also a graduate teaching assistant and a research assistant. Some courses that she taught as a graduate teaching assistant included Principles of Biology for non-science majors, General Biology 1 for science majors, and Microbiology laboratory classes for pre-health majors. Also, in January 2010, Ijeoma presented some of her research findings at the Society for Integrative and Comparative Biology conference held in Seattle, WA. Currently, Ijeoma is working as a Laboratory Technician at the University of North Florida's physiology laboratory and plans on pursuing a Ph.D in Biomedical Sciences.